DEVELOPMENT OF A COMPETITIVE RT-PCR ASSAY TO EXAMINE A1 EXPRESSION IN BURSAL LYMPHOCYTES

by

ANGELA LAURA BURRELL

(Under the Direction of Mark M. Compton)

ABSTRACT

The A1 differential display product was initially isolated from thymocytes undergoing apoptosis, and its expression was shown to increase as function of time in this model system. In the current research, a more sensitive technique, the Competitive RT-PCR assay, was employed to examine the expression of the A1 gene in bursal lymphocytes undergoing apoptosis. This line of investigation demonstrates that there is a surge in A1 expression during the initial phases of apoptosis, indicating that A1 may represent a critical activation signal in the apoptotic cascade. Furthermore, this study indicates that agents known to inhibit apoptosis in bursal lymphocytes, such as the phorbol ester PDBu, also function to moderate A1 expression. Since PDBu activates the protein kinase C-signaling pathway, this finding suggests a possible link between A1 and the protein kinase C pathway.

INDEX WORDS: Apoptosis, A1 Differential Display Product, Bursal Lymphocytes, Competitive RT-PCR, Phorbol Ester

DEVELOPMENT OF A COMPETITIVE RT-PCR ASSAY TO EXAMINE A1 EXPRESSION IN BURSAL LYMPHOCYTES

by

ANGELA LAURA BURRELL

B.S.A, The University of Georgia, 2001

A Thesis Submitted to the Graduate Faculty of The University of Georgia in Partial Fulfillment of the Requirements for the Degree

MASTER OF SCIENCE

ATHENS, GEORGIA

2003

DEVELOPMENT OF A COMPETITIVE RT-PCR ASSAY TO EXAMINE A1 EXPRESSION IN BURSAL LYMPHOCYTES

by

ANGELA LAURA BURRELL

Major Professor:	Mark M. Compton
Committee:	Adam J. Davis William A. Dozier, III

Electronic Version Approved:

Maureen Grasso
Dean of the Graduate School
The University of Georgia
August 2003

DEDICATION

This work is dedicated to my best friend David Waldroup and to my parents, Bill and Sheila Burrell. Your love and support have paved the way for my accomplishments.

ACKNOWLEDGEMENTS

I am deeply grateful to the many people who have helped me to reach this place in my academic career. From my parents to my friends along the way, you have encouraged me and built in to me many things that have helped me reach this point.

Specifically, I would like to thank Dr. Compton who has guided me through the process of gaining a MS degree and whose last minute efforts were instrumental in allowing me to graduate during summer semester. I appreciate the knowledge and experience you imparted to me.

Dr. Davis, thank you for all the practical advice you have given me along the way and for helping me successfully navigate many unknown roads.

Thank you Dr. Dozier for the feedback you have given me in this process and also for the opportunity to work on your experiment.

Marvin, the pictures in my thesis look great! I truly appreciate your assistance in preparing them so quickly.

Thank you Dr. Lacy for giving me your personal support throughout my time here. I hope this department realizes how valuable your leadership is!

Dr. Fairchild, thank you for all that you have done. From getting birds to preparing PowerPoint slides, you have always been eager to assist me.

Thank you Lorraine for continually providing me with birds for my experiments. I certainly would not have graduated this semester without your help.

A special thanks to my brother Billy for going out of his way to fulfill my technology needs. You are one of the nicest people I know!

To David Waldroup, thank you for standing by me during this process. Your valiant efforts have meant so much and your sacrifices will never be forgotten.

Finally, I want to thank my Lord and Savior Jesus Christ. For I have come to truly understand that, "His grace is sufficient for me, and His strength is made perfect in weakness." To have a relationship with Jesus Christ is to experience the greatest peace and joy that humanity can know. If only everyone could be that rich!

TABLE OF CONTENTS

Page

LIST OF TABLES

Page

LIST OF FIGURES

Page

CHAPTER 1

INTRODUCTION

The Role of Apoptosis

Since its initial characterization, apoptosis has been shown to play a vital role in diverse cellular processes impacting virtually all multicellular organisms. In many species, apoptosis is responsible for the demise of autoreactive lymphocytes that arise during the development of B and T cells (1). Within peripheral lymphoid organs, apoptosis then functions to regulate the activation of mature B and T cells that participate in the immune response. In addition, apoptosis is a crucial component in the morphological development of various body structures, ranging from the deletion of cells that form the interdigital webbing of the hands and feet during embryogenesis to the death of myocardial cells during the development of the embryonic chick ventricle (2).

In addition to its role in embryogenesis and immune function, apoptosis also plays a role in the development of various diseases processes. Specifically, inadequate or deficient apoptosis may instigate cancer in response to decreased levels of p53, a cellular protein which functions as a transcription factor that regulates genes involved in DNA repair and cell division (3). Although the native conformation of p53 typically triggers apoptosis, a mutation of a single nucleotide may lead to a lack of cell death that, in turn, promotes cancer. In another diseases process, acquired immune deficiency syndrome (AIDS), T cells become infected with the human immunodeficiency virus (HIV), which activates the apoptotic process and results in the depletion of T helper lymphocytes (4).

Much of the current research regarding apoptosis is focused on understanding the regulation of the cell's apoptotic machinery within various organisms, with the hope that this knowledge will provide insights into the prevention and treatment of diseases that are triggered by cell death. In pursuit of this knowledge, researchers have discovered that different organisms posses similar genes which mediate apoptosis. For example, homologous gene sequences of the Caspase Gene Family have been documented in various mammalian species, as well as in *C. elegans* and *Drosophilia* (2). Furthermore, while the concept of programmed cell death is well accepted in multicellular organisms, it has also been recently described in some unicellular organisms, including *Trypanosomatids* (5-6) and *Leishmania* (7-8). Nevertheless, the existence of apoptosis in unicellular organisms remains controversial since these organisms differ in their response to apoptosis inhibitors and because they lack the characteristic morphological and biochemical features of apoptosis (9).

Morphology of Apoptosis

Although cell death has long been studied, the term apoptosis was not coined until 1972. Researchers during this time observed a unique form of cell death in various tissues and cell types that shared common morphological features (10). They utilized these unique morphological characteristics to distinguish apoptosis from necrosis, which is an accidental form of cell death that is initiated by a physiological stress and activates an inflammatory response (11-12). Hence, apoptosis has now been classified as a form of signal-induced cellular suicide where a target cell activates a genetic program that brings about its own destruction (13-15).

During the initial phase of the apoptotic process, cells shrink and disconnect from neighboring cells. This is followed by cell blebbing and condensing of the chromatin, which is a direct result of alterations in DNA and histone interactions (4). These changes are accompanied by modifications in the DNA itself, including both single-stranded and two types of double-stranded DNA breaks. One type of double-stranded DNA break results in the formation of high-molecular-weight DNA fragments, which may occur after glucocorticoid or etoposide treatment of cells. These large DNA fragments are generated by the cleavage of chromatin from the nuclear scaffold. The second type of double-stranded DNA break involves the cleavage of the DNA into 180 bp fragments, forming one of the hallmarks of apoptosis, the "DNA ladder," which can be visualized by agarose gel electrophoresis. The generation of these smaller DNA fragments is mediated by nucleases that selectively cleave DNA between nucleosomal units. Recent evidence suggest that DNA fragmentation factor (DFF)/caspase-activated DNase (CAD) is the primary nuclease responsible for DNA fragmentation in apoptotic cells (16-17).

In conjunction with the nuclear events associated with apoptosis, a number of other cellular events accompany this form of programmed cell death. For instance, apoptotic cells present phosphatidylserine (PS) on the outer cell membrane, which enables phagocytes to recognize and dispose of them in the later stages of apoptosis without eliciting an inflammatory response (4, 18). The externalization of PS occurs early in the apoptotic process and is believed to be caused by an increase in the calcium-activated enzyme "scramblase" and a decline in aminophospholipid translocase activity.

Genetic Mediators of Apoptosis

From the onset of signaling to the terminal phase of cellular destruction, apoptosis is a complex process with multiple layers of regulation. Although the intricate mechanisms of this phenomenon remain somewhat obscure, current insights into the apoptotic process reveal four families of gene products that are primarily responsible for mediating cellular death: Death Receptors, Adaptor Proteins, Caspases, and Bcl-2 Proteins (19-20, 22). Members of these gene families interact to promote and regulate the apoptotic process at various points along the signal transduction pathway.

Death Receptor Gene Family

Death receptor-mediated apoptosis involves the binding of a ligand to the external domain of a Death Receptor, enabling the apoptotic signal to reach the cytoplasmic portion of the cell. Death receptors are type-I transmembrane proteins that possess a membrane-spanning region, a N-terminal domain that binds extracellular ligands, and a C-terminal intracellular tail (Figure 1) (21). All members of the Death Receptor Gene Family share significant homology in their ligand-binding region, which typically contains 1-5 cysteine-rich domains. The intracellular death domain (DD) is responsible for triggering the death signal, and it is characterized by a homologous 60-80 amino acid sequence. Currently, six death receptors possessing death domains have been identified, including Fas, TNF-R1, DR3, DR4, DR5, and DR6 (Table1) (22-24).

Adaptor Protein Gene Family

In response to the Death Receptor/ligand interaction, an Adaptor Protein binds to and simultaneously recruits the upstream components of the caspase-signaling cascade to further promote apoptosis. In general, adaptor proteins contain modular domains that

allow them to intercede in protein-protein and protein-lipid interactions, and they are responsible for bringing effector and target proteins into close proximity with each other (25). To date, many adaptors have been implicated in various biological processes, such as lymphocyte development and immune cell activation. The most common adaptors associated with apoptosis are FADD, TRADD, RIP, FLIP, and TRAF2 (Table 2) (22-23, 26-27).

Caspase Gene Family

Following the adaptor-mediated interaction between the Death Receptor and upstream caspase components, a proteolytic signaling cascade is activated and subsequently activates downstream effector caspases. The proteolytic activity of these effector caspases inactivates cellular repair mechanisms and promotes the morphological changes that accompany apoptosis. This caspase signaling cascade is a complex pathway that represents the primary mechanism of cell death; however, there is other evidence of caspase-independent cell death in cases where the cell is severely compromised during autophagy and proteasomal degradation (28).

Constituents of the Caspase Gene Family are cysteine proteases that cleave substrates after an Asp residue, hence the origin of their name: cysteine-dependent aspartate-specific protease (29). Caspases operate as specific proteases, with each caspase recognizing a specific sequence of four amino acids. Given their preference for Glu and Asp at positions 3 and 1 respectively, the general caspase specificity can be described as X-Glu-X-Asp (X-E-X-D). Caspases are synthesized as catalytically inactive zymogens, which are subject to proteolytic processing during apoptosis (30). At present, 14 mammalian caspases have been identified and classified as either initiator

caspases or effector caspases (Table 3) (29, 31-32). An extended N-terminal prodomain of at least 90 amino acids distinguishes initiator caspases from effector caspases, the latter having only 20-30 amino acid residues in their prodomain sequence. Initiator caspases are autoactivated upstream of effector caspases and subsequently trigger the activation of downstream effector caspases. These activated effector caspases are ultimately responsible for executing programmed cell death. Once activated, the effector caspases cleave a range of cellular substrates, including the structural components actin and nuclear lamin, as well as regulatory proteins, such as DNA-dependent protein kinases.

At the N-terminal region of initiator caspases and caspases-1, -4, and -5, two types of non-catalytic domains are present: CARD (caspase recruitment domain) and DED (death effector domain) (29). During activation, these domains are cleaved and the active, catalytic portion is released (with the exception of caspase-9). Release of this catalytic portion of the initiator caspase permits the proteolytic activation of downstream effector caspases. Less is known about whether the effector caspases contain similar types of non-catalytic domains, although the amino acids within the N-terminal region appear to be removed during the activation process. Moreover, all members of the caspase family demonstrate immense similarity in regard to their catalytic units, each containing both a large (approximately 20 kDa) and a small (approximately 10 kDa) domain. For pro-caspases to be activated, it is essential that the two subunits dimerize and undergo proteolytic processing. This proteolytic caspase cascade is triggered by initiator caspases, which activate intermediate caspases that, in turn, activate executioner caspases.

Since the initiator caspases are devoid of upstream proteases, how are these caspases activated? This mechanism is currently unknown, although one theory, the induced proximity model, proposes that initiator caspases are recruited to protein complexes whose formation increases the local concentrations of caspase zymogens. Since these zymogens contain low levels of inherent enzymatic activity, the clustering of zymogens may allow for activation of the first protease(s) in the casacade (33). At each step along the cascade, various proteins are known to participate in caspase regulation. Notably, FLIP (Flice-like inhibitory protein), CrmA, and members of the IAP (inhibitor of apoptosis protein) family are among the well-recognized inhibitors of caspases (29).

Bcl-2 Gene Family

Another point of regulation along the caspase cascade involves the Bcl-2 Gene Family. When the upstream caspases are activated, they promote the activation of Bcl-2 proteins, which characteristically alter mitochondrial function and allow for the activation or inhibition of downstream caspases via regulation of caspase-9 (34). Members of the Bcl-2 Gene Family are classified as either anti-apoptotic (inhibition of apoptosis) or pro-apoptotic (stimulation of apoptosis) (Table 4) (35-36). Among the members of the Bcl-2 Gene Family, there are four homologous regions known as Bcl-2 homology (BH) domains (35). Typically, the anti-apoptotic proteins contain all four domains, requiring BH1, BH2, and BH4 in order to inhibit apoptosis. These proteins also contain a hydrophobic domain (HCD) within their C-terminal region, which is believed to participate in directing the proteins to intracellular membranes. Conversely, some pro-apoptotic Bcl-2 proteins also contain a C-terminal hydrophobic domain, whereas other pro-apoptotic Bcl-2 proteins like Bid and Bad lack this domain. All pro-apoptotic

members of the Bcl-2 Gene Family, however, possess a BH3 domain that is necessary for their apoptotic activity. In addition to the BH3 domain, some pro-apoptotic proteins, such as Bax, Bak, Bok, and Bcl-X_s, contain other BH domains. A new member of the pro-apoptotic family was recently identified and named Bcl-2 rambo. This protein is unique because it contains all four BH domains, as well as a novel C-terminal extension that is required for the promotion of apoptosis, instead of the BH3 domain that is required by the other pro-apoptotic family members.

It has been reported that the activity of Bcl-2 proteins is regulated by formation of homodimer and heterodimer complexes between the hydrophobic groove of anti-apoptotic proteins and the amphipathic BH3 α-helix of pro-apoptotic Bcl-2 proteins (34). Thus, the relative concentrations of anti-apoptotic and pro-apoptotic proteins influence whether a cell will undergo apoptosis. For instance, increased levels of Bad foster heterodimer formation between Bad (pro-apoptotic) and Bcl-x_L (anti-apoptotic), which enables Bax (pro-apoptotic) to be released and bind to Bcl-2 (anti-apoptotic), thereby promoting cell death (37). Furthermore, post-translational modifications, such as proteolysis and phosphorylation, in "BH3 domain only" proteins may alter the relative affinity between anti-apoptotic and pro-apoptotic proteins, therefore regulating the formation of homodimer and heterodimer complexes. For example, cytokine-induced phosphorylation of Bad via protein kinase A and Akt inhibits apoptosis (1). In this scenario, phosphorylated Bad is sequestered by the phosphoserine-binding protein, 14-3-3, and thereby inactivated. Alternatively, the withdrawal of cytokine signals for cells may induce apoptosis via dephosphorylation of Bad.

Extrinsic Pathway of Apoptosis

Although apoptosis can be triggered by a wide variety of stimuli, the signal transduction pathways can be divided into two predominant types, the extrinsic and intrinsic pathways (Figure 2) (21, 31). The extrinsic pathway is induced by stimuli at the cell surface, typically involving death receptor ligands, and is frequently referred to as the death receptor pathway. Conversely, in the intrinsic pathway, apoptosis is initiated by a disturbance in intracellular homeostasis, which can be triggered by cell damage pathways such as irradiation and growth factor deprivation. Since the mitochondria are essential for execution of cell death in the intrinsic pathway, it also known as the mitochondrial cell death pathway.

Among the death receptors that have been described, perhaps the best understood extrinsic pathway is that involving the Fas receptor, which belongs to the Tumor Necrosis Factor Receptor (TNF-R) family of death receptors (38). In this signaling pathway, Fas Ligand binds to the Fas receptors, which are expressed on the cell surface of activated T lymphocytes and induces apoptosis. This pathway is activated in virus-infected cells and cancer cells, and it appears to play a role in the homeostatic maintenance of T and B cell populations (21). Binding of the Fas Ligand activates the death receptor complex and enables the adaptor protein, Fas Associated Death Domain (FADD), to bind to the intracellular domain of Fas (22, 39). Death domains (DD) in the amino terminal region of FADD and in the cytoplasmic region of Fas bind in a homotypic fashion to generate a Fas Ligand/Death Receptor complex. This interaction results in the formation of the Fas Receptor/FADD Adaptor complex, also referred to as the death-inducing signaling complex (DISC), which initiates procaspase-8 binding to the adaptor protein through

mutual death effector domains (DED) in the C-terminal region of FADD and the N-terminal region of procaspase-8. When procaspase-8 is recruited to FADD, an autoproteolysis step is initiated, resulting in the activation of caspase-8 (22). In turn, this prompts the activation of downstream effector caspases (capsase-3, -6, and -7) and results in the characteristic apoptotic phenotype – degraded cytoskeleton proteins (40) and nuclear lamina (41). In addition, the downstream effector caspases trigger the nuclease activity responsible for internucleosomal cleavage of DNA (17).

Caspase-8 has long been considered as the primary initiator caspase for the Fas receptor pathway, yet recent literature indicates that caspase-10 may also function in the initiation process (42-43). Research demonstrates that caspase-8 and caspase-10 can function independently of one another, yet the kinetics for DISC recruitment and processing of both caspases appear indistinguishable from each other. Furthermore, caspase-10 is highly expressed in primary cells derived from the immune system, and the studies suggest that caspase-10 is activated by self-aggregation, similar to the induced proximity model for caspase-8 activation.

Another recent study suggests that there are two types of cell lines that engage in distinctive CD95 (Fas) signaling pathways (44). When apoptosis was induced in type I cells, large amounts of DISC were generated and directly activated caspase-8, without inhibition of cell death by Bcl-2 proteins. In contrast to type I cells, activation of apoptosis in type II cells was accompanied by a reduction in DISC formation and Bcl-2 proteins were shown to directly regulate the apoptotic process. In addition, there was evidence that caspase-8 was not activated in type II cells until after modifications in the mitochondrial transmembrane potential had occurred. However, both types of cell lines

demonstrate similar kinetics of CD95-mediated apoptosis and both resulted in similar mitochondrial changes. Therefore, the differences in these two cell lines cannot be attributed to opposing means of mitochondrial activation; rather, they may differ in their relative dependence on the mitochondria in the apoptotic cascade.

At present, only a limited number of cells have been classified as type I or type II cells (31). Among these, peripheral T cells and thymocytes are characterized as type I cells, whereas the liver and possibly neurons are described as type II cells. While apoptosis in type I and type II cells are both stimulated by ligand binding to the death receptors, the Bcl-2 family of proteins regulates the Fas pathway by activating the downstream effector caspases via mitochondrial involvement following the binding of FasL to the Fas death receptor in type II mammalian cells (45). Hence, the extrinsic pathway in type II cells recruits an intrinsic, mitochondrial pathway. Once caspase-8 is activated in the death receptor pathway, it cleaves the Bcl-2 protein Bid, yielding a truncated Bid (tBid) that subsequently binds to mitochondrial-bound Bcl-2 (Figure 2). Binding of tBid to Bcl-2 inhibits the anti-apoptotic activity of Bcl-2 and promotes the release of cytochrome c from the mitochondria. Cytochrome c then combines with procaspase-9, dATP, and Apoptosis Activation Factor (Apaf-1) to form a complex termed the apoptosome (46). Formation of the apoptosome enables the activation of caspase-9, which allows the downstream effector caspases-3, -6, and -7 to be activated as well.

Anoikis, the loss of cell anchorage, has been shown to induce apoptosis and may also be related to the Fas-receptor mediated signaling pathway (47). When anoikis occurs in human endothelial cells, it leads to an increase in Fas and Fas-Ligand

expression, while dramatically downregulating FLIP, an endogenous inhibitor of this pathway. Furthermore, activation of the death receptor pathway may be a result of a positive feedback mechanism. When intestinal epithelial cells undergo anoikis, caspase-2, caspase-9, and cytochrome c are activated prior to activation of caspase-8. Although the genetic mediators of anoikis are unknown, it appears that cellular detachment is a critical event in the apoptotic pathway of some cell types.

Intrinsic Pathway of Apoptosis

Unlike the Fas pathway, the intrinsic, or mitochondrial pathway, has only recently been described in terms of its contribution to apoptosis, and to date, its mechanisms are less clear. Originally, collapse of the mitochondrial transmembrane potential, caused by an uneven distribution of protons on both sides of the inner mitochondrial membrane, was proposed to activate this pathway and was considered to be an irreversible step in apoptosis (48). It is now believed that cytochrome c, an electron shuttle molecule that participates in the oxidative phosphorylation pathway, is responsible for activating the caspases that execute apoptosis (34). Although it has been shown that the disruption of the mitochondrial transmembrane potential participates in apoptosis, it has also been demonstrated that, in some cases, cytochrome c release from the mitochondria occurs in the absence of transmembrane potential collapse (49-51).

Activation of the intrinsic pathway resembles the mitochondrial component of the extrinsic pathway, since it involves the release of cytochrome c from the mitochondria and the formation of the wheel-shaped apoptosome (Figure 2). The apoptosome possesses sevenfold symmetry and is comprised of cytochrome c, procaspase-9, dATP, and Apoptosis Activation Factor (Apaf-1) (46, 52). Formation of the apoptosome

triggers the activation of caspase-9, allowing the downstream effector caspase-3, and -7 to be activated as well. In turn, this promotes the activation of caspase-2, -6, -8, and -10, which results in positive feedback signals that perpetuate the apoptotic cascade (34).

It is undisputed that Bcl-2 proteins regulate apoptosis at the level of the mitochondria via the formation of homo and heterodimers between anti-apoptotic and pro-apoptotic proteins. Nevertheless, much controversy exists regarding the means by which this occurs at the molecular level. One model suggests that opening of the permeability transition pore (PTP), a protein complex present at interaction sites between the inner and outer mitochondrial membranes, results in the collapse of the transmembrane potential, allowing for the release of proteins such as cytochrome c (53). It has been postulated that members of the Bcl-2 Gene Family regulate the opening of the PTP by interacting with components of the inner and outer mitochondrial membranes, including the adenine nucleotide translocator (ANT) and the voltage-dependent anion channel (VDAC) (34). Pro-apoptotic proteins such as Bax and Bak are believed to induce PTP opening, whereas anti-apoptotic proteins, including Bcl-2 and Bcl-x_L, prevent the opening of the PTP.

Alternatively, a second model postulates that pro-apoptotic Bcl-2 proteins form tetrameric channels that enable the release of proteins from the innermembrane space of the mitochondria. Following the translocation of tBid to the mitochondria, it has been shown that tBid promotes the release of cytochrome c without disrupting the transmembrane potential (50-51). Furthermore, tBid may also trigger the translocation and oligomerization of Bax and Bak in the outer mitochondrial membrane, enabling Bax and Bak to form ion channels (34). In contrast, anti-apoptotic proteins inhibit the

conformational change and oligomerization of Bax and Bak, and thereby prevent the formation of ion channels and the release of cytochrome c. Other pro-apoptotic proteins, such as Bad and Bim, bind to anti-apoptotic Bcl-2 proteins and induce a conformational change that transforms the anti-apoptotic activity of these proteins to that of pro-apoptotic proteins involved in promoting apoptosis via ion channel formation within the mitochondria.

Another constituent of mitochondria-activated apoptosis is the role of calcium ions (Ca^{2+}) in the signal transduction pathway (54). Under normal conditions, Ca^{2+} cycles between the mitochondria and the endoplasmic reticulum (ER) by employing the sarcoplasmic reticulum calcium ATPases (SERCA) that pump calcium ions into the ER. An overexpression of SERCA increases levels of Ca^{2+} in the ER and sensitizes the cells to apoptosis. Research has linked the balance of anti-apoptotic and pro-apoptotic Bcl-2 proteins with the modulation of Ca^{2+} load in the ER. For instance, increased levels of Bcl-2 decreases the Ca^{2+} content of the ER, thus protecting the cells from apoptosis. Conversely, cell death is induced when there are substantial levels of Bax and Bak, which promotes the movement of Ca^{2+} into the mitochondria and may form tetrameric channels in the mitochondrial membrane that promote the apoptotic cascade. Although there is clearly a correlation between the levels of Ca^{2+} in the ER and the mitochondria and their effect on apoptosis, the mechanisms dictating these interactions are not completely understood at this time.

Interactions of Cellular Pathways that Regulate Apoptosis

In addition to the death receptor signaling pathway, numerous other cellular mediators act on the mitochondria to induce apoptosis, including ceramide, growth

factors, and cellular products generated during irradiation. Ceramide is a membrane sphingolipid that is involved in cell differentiation, proliferation, and cell death (55-56). This sphingolipid is generated by various cellular processes, such as the hydrolysis of sphingomyelin and metabolic reactions involving sphingosine. Additionally, there is a *de novo* pathway of ceramide synthesis that is activated in response to chemotherapeutic agents, Fas ligand, and TNF death receptor signaling, which leads to an elevation in the levels of intracellular ceramide and the induction of apoptosis. Recent research suggests that ceramide may exert its apoptotic effect upstream of Bcl-2 and executioner caspase-9 and -3 (57-58). Other evidence indicates that ceramide has downstream actions involving the regulation of the Bcl-2 proteins at the level of the mitochondria (59).

Several growth factors have been shown to influence the mitochondrial activation pathway of apoptosis. For example, treatment of myeloid cells with the hormone IGF-1 and cytokines IL-3 and IL-4 enhances cell survival by inhibiting capsase-3 activation (60). In the absence of these factors, caspase-3 activation occurs and apoptotic cell death ensues via the caspase signal transduction cascade. Furthermore, recent research has indicated that growth factor withdrawal from IL-3-dependent lymphoid cells results in a disruption in mitochondrial respiratory control (61). Specifically, this process impairs the ADP/ATP cycle that is necessary for ion exchange, and leads to the overproduction of reactive oxygen species (ROS), which elicit the activity of apoptotic mediators and promote cell death (62).

Moreover, growth factor deprivation also plays a role in cellular pathways involving p53, a tumor suppressor protein that functions as a transcriptional factor to regulate cell growth, DNA repair, and apoptosis (3). Elevated levels of p53 are generated

following DNA damage and act as transcriptional activators to increase the expression of pro-apoptotic Bcl-2 proteins, such as Bax and Noxa (22, 63). These pro-apoptotic proteins promote apoptosis by triggering the release of cytochrome c from mitochondria. Furthermore, p53 also engages in the extrinsic pathway by upregulating the expression of Fas and DR5 Death Receptors. Interestingly, this p53-mediated induction of death receptor expression can be accompanied by an activation of these receptors in the absence of ligand binding. Nevertheless, with the addition of cytokines, namely IL-6, p53-dependent apoptosis can be suppressed in myeloid cells (64).

When cells are exposed to irradiation, it promotes apoptosis by simultaneously activating multiple signaling pathways, including the mitogen-activated protein kinase (MAPK) cascade (65). The MAPK pathway consists of several cascades that are characterized by protein kinase activity (66), including the JNK pathway that is believed to participate in TNF induced apoptosis (67). In addition to irradiation, ceramides and growth factors can also stimulate MAPK activity and, in turn, promote apoptosis.

Although apoptosis is a natural and often beneficial process, it must be held in balance by cellular pathways that encourage cell survival. One means of promoting survival is through the NFκB Kinase Cascade, which collectively comprises several transcription factors that play a role in inflammation and regulation of the immune response (38). In most cells, these factors exist in a latent form due to their association with I-κB inhibitory proteins that influence their cytoplasmic location. After interacting with TNF receptors, and in some cases CD95, certain I-κB proteins undergo phosphorylation, which leads to the activation of NFκB. Subsequently, NFκB translocates to the nuclease and initiates transcription of genes that participate in cell

survival pathways (21). Conversely, inhibition of NFκB makes the cells vulnerable to TNF-induced apoptosis.

While the extrinsic and intrinsic pathways, as well as the many other pathways that influence cell death, are initiated by different mechanisms, they ultimately converge to produce the characteristic morphological and biochemical alterations of apoptosis. Furthermore, there is evidence that several of these pathways communicate upstream of this convergence point. Thus, while these pathways are often described separately for simplification, in reality, they are integrated in a complex manner, with the extent of their relationship remaining a tangled web that has yet to be unraveled.

A1 Gene

A number of techniques have been employed to identify genes involved in apoptosis, including the differential display methodology (68), which involves amplification of cDNAs using arbitrary primers. In our laboratory, thymocytes were treated with a glucocorticoid to induce apoptosis and the differential display technique was used to identify a 479 bp product designated as A1 (69). An autoradiograph demonstrating A1 expression at zero, one, and four hours following dexamethasone treatment showed that its expression increased with time (Figure 3).

Furthermore, a ribonuclease protection assay (70) was used to confirm that A1 expression was induced as a function of the apoptotic process (69). Thymocytes were treated with either dexamethasone (a glucocorticoid) or A23187 (a calcium ionophore) over a 0 to 6 hour time period. Both treatments revealed that A1 expression increased as a function of time, with approximately a two-fold increase following dexamethasone treatment and a six-fold increase following A23187 treatment (Figure 4).

These preliminary data have provided potential insights into the role of the A1 gene in apoptosis. Since A23187 dramatically stimulates A1 expression in thymocytes, this gene may be regulated by means of an intracellular calcium-signaling pathway. Moreover, these data indicate that A1 may be induced during the early phase of apoptosis. When a nucleotide sequence analysis was performed (Figure 5) (69), it revealed that A1 possesses a putative 82 amino acid open reading frame, which shares limited homology with Bad (Figure 6), a pro-apoptotic regulatory protein belonging to the Bcl-2 family.

mRNA Quantitation

In the current work, we were interested in using Competitive RT-PCR methodology to analyze the expression of A1 in bursal lymphocytes. Diverse techniques have been used historically to measure mRNA expression, including Northern blots, dot blots, and ribonuclease protection assays. Northern analysis (71) begins with the separation of mRNA via denaturing gel electrophoresis, which is followed by transferring the RNA of interest onto a membrane matrix via capillary action. A radiolabeled probe is hybridized to the immobilized RNA on the membrane matrix. Autoradiography is then performed to quantitate the hybridization signal. Dot blot analysis (72) resembles Northern blot analysis, except that dilutions of the RNA samples are applied directly onto a membrane under a negative pressure using a multiwell apparatus. Once the image is captured by autoradiography, the degree of hybridization is quantitated by scanning densitometry. As compared to dot blot analysis, Northern analysis is advantageous because it provides an indication of the relative size of mRNA.

Another technique that is used for mRNA quantitation is the ribonuclease protection assay (70), which also involves hybridizing a radiolabeled probe to the RNA samples. However, this hybridization step occurs in solution. The RNA is then subjected to RNase digestion, in which the hybridized strands are protected from RNase action. The products are subsequently electrophoresed on a denaturing polyacrylamide gel (PAG) and autoradiography is performed to view the results. While Northern blot analysis, dot blot analysis, and the ribonuclease protection assay are suitable for mRNA quantitation, they require relatively large amounts of RNA and are less sensitive than newer methodologies that utilize reverse transcription and the polymerase chain reaction (RT-PCR) methodology to quantitate mRNA.

Competitive RT-PCR

One popular technique that is currently used to quantitate gene expression is Competitive RT-PCR, which is variously termed RNA-phenotyping (73), RNA-PCR (74), and message amplification phenotyping (75). The interest in this technique for mRNA quantitation has increased because Competitive RT-PCR, unlike other methods, enables the investigator to simultaneously examine many samples and/or many different genes within the same sample (76). Furthermore, since it requires small amounts of RNA, Competitive RT-PCR is a sensitive technique that permits gene expression analysis of rare transcripts (76), such as A1.

Competitive RT-PCR involves six basic steps: RNA isolation, conversion of RNA to cDNA via Reverse Transcriptase, amplification by the Polymerase Chain Reaction (PCR), agarose gel electrophoresis analysis of PCR products, and quantitation of the target RNA using an exogenous standard. Quantitation of mRNA using the Competitive

RT-PCR technique relies on coamplification of a "standard" with the target gene in a PCR reaction, thus fostering competition between the target and the standard for binding of the PCR primers. To perform this competition reaction, the standard must possess similar amplification efficiencies as the target and both should contain the same primer template sequences. When Competitive RT-PCR was initially described (77-78), two types of standards were used that differed slightly in size from the target gene. The first type of standard was a genomic fragment of the gene of interest that contained a small intron that produced a larger PCR product as compared to the target transcript. Alternatively, a slightly smaller PCR standard could be generated by engineering a cDNA with a unique restriction enzyme site that was digested with a restriction enzyme prior to electrophoretic analysis. These minor modifications in size enabled the standards to be distinguished from the target without altering the amplification efficiency. Using these types of standards, Competitive RT-PCR was performed by adding various dilutions of known amounts of the standard into a series of PCR reaction tubes all containing equal amounts of the target cDNA.

Since the initial description of Competitive RT-PCR, many variations of this technique have been developed. For instance, some researchers have reported adding dilutions of the target to a fixed amount of the standard (79), whereas others investigators have added the internal standard at the reverse transcription reaction rather than the PCR reaction (80). Recently, a serial RT-PCR strategy has been developed that involves adding a series of standards with different sizes and concentrations into one tube containing a known amount of total RNA (81). This method is advantageous because multiple RNA standards can be coamplified with the target RNA in a single tube.

Traditionally, HPLC (82) or gel electrophoresis (83) has been used as an "end-point" to measure the accumulation of PCR products. However, a more efficient method known as "real-time" PCR, or Kinetic PCR, has been implemented in the quantitation of mRNA levels (84). This technique involves the use of a gene specific "TaqMan" probe that consists of two fluorescent dyes, a 5' reporter dye and a 3' quencher dye. As long as the probe integrity is maintained, the quencher dye quenches the reporter dye fluorescence due to its physical proximity to the quencher dye. However, during PCR amplification, the reporter dye is cleaved and thereby enables its fluorescent quantitation with each PCR cycle. The exponential accumulation of the reporter dye during PCR amplification is proportional to the initial amount of the target gene. Although "real-time" PCR is a powerful tool for mRNA quantitation, the expense of both the equipment and the probes limits its use for some laboratories.

Development of a Competitive RT-PCR Assay to Quantitate Gene Expression

Since the Competitive RT-PCR methodology is both cost efficient and sensitive, we used this assay for mRNA quantitation of A1. Development of a Competitive RT-PCR assay involves a series of steps, starting with the isolation of total RNA. There are a variety of ways to isolate RNA, but a common method involves the use of a guanidinium lysis buffer (85). This solution is a chaotropic agent that disrupts cells, while simultaneously inactivating RNases by inhibiting their tertiary structure, thus RNases cannot compromise the integrity of the RNA sample while in solution. More recently, the acid-guanidinium thiocyanate-phenol-chloroform extraction (86) technique was developed as an efficient method for RNA isolation that enables the investigator to simultaneously isolate DNA, RNA, and protein from the same biological source.

Although the guanidinium thiocyanate method is very effective for RNA isolation, minute amounts of DNA contamination may persist. If present in the RNA sample, DNA contamination may contribute to an overestimation of mRNA expression using the Competitive RT-PCR methodology. For more accurate results, RNA samples should be treated with RNase-free DNase prior to RT-PCR (87).

In addition to the target RNA preparation, a standard must be generated for Competitive RT-PCR assays. Many different types of standards have been reported (88-90), but RNA standards are advantageous since they can be added to the reverse transcription reaction. Homologous, external standards are especially beneficial because they share the same primer binding sites as the target RNA, are most likely to share similar RT and PCR efficiencies, and have the same sequence, except for a minor mutation, insertion, or deletion (76). Typically, homologous standards are created by inserting the standard cDNA into a plasmid, which contains a RNA polymerase promoter that permits the in-vitro transcription of RNA standard transcripts. An insertion or deletion of approximately 10% (91) is made to distinguish the standard RNA from the target RNA (88).

Following RNA preparation, treatment with DNase, and construction of the RNA standard, a reverse transcription reaction is performed to produce a single-stranded complementary DNA copy (cDNA) of the RNA (92) using Reverse Transcriptase, a retroviral enzyme that has RNA-dependent DNA Polymerase activity (76). An oligonucleotide primer, such as oligo $(dT)_{12\text{-}18}$, is added to the reaction to initiate cDNA synthesis (76). Once this primer anneals to the polyadenaylated 3' tail of mRNA, the cDNA is lengthened toward the 5' end of the mRNA via Reverse Transcriptase. To

normalize this reaction among samples, both the target RNA and the standard RNA are added together in this reaction to enhance quantification of the target mRNA. Due to the incredible sensitivity of the Competitive RT-PCR technique, small amounts of RNA can be added to the reverse transcription reaction. There are reports indicating that amounts as little as 0.5 attomol of target RNA can be detected by Competitive RT-PCR (93).

The polymerase chain reaction (PCR) (94-95) is used to exponentially amplify the cDNA product. It is performed with successive cycles, each cycle consisting of three fundamental components: sample denaturation, annealing of the primers, and elongation. The denaturation step is performed at temperatures as high as 94°C to separate the double stranded template so that primer binding is facilitated. In the annealing step, the primers hybridize to the template within the range of 42-65°C, depending on the melting temperature (T_m) of the primers. A vital component of the annealing step is the primer design, which is specific for the target and defines the size of the PCR product. Many rules govern the design of adequate primers, namely the primers should share similar T_m and possess approximately a 50% GC content (96-97). The two primers used for PCR are the upstream (forward) primer, which binds to the newly synthesized first strand cDNA, and the downstream (reverse) primer, which binds to the 3' end of the RNA template. Finally, the elongation step occurs between 68-72°C and relies on Taq Polymerase, a thermostable DNA Polymerase isolated from *Thermus aquaticus* (97). Since this enzyme is active at very high temperatures, it is ideal for PCR amplification.

The accumulated PCR product must subsequently be separated so that the standard and the target can be differentiated and quantified. As mentioned previously, there are multiple techniques that can be used for "end-point" measuring, including

HPLC and agarose gel electrophoresis. Agarose gel electrophoresis (83) is among the most traditional means of detecting PCR products for quantitation, as it provides suitable resolution and is relatively easy to perform. Following gel electrophoresis of the samples, the gel is densitometrically scanned to obtain quantitative values for the target and the standard PCR products. These values are then used to determine the ratios of the target and standard, which are plotted on a double log scale graph against the amount of standard added to the reverse transcription reaction. The relative amounts of PCR products generated are dependent upon competition between the target and the standard for PCR primers. Hence, the ratio between the standard and the target templates can be used to estimate the amount of initial target in the sample when the amount of added standard is known. Accordingly, as the amount of the standard levels increase, the amount of the target signal decreases. Quantitation is then determined using the point where the target and the standard ratio equal one, and ideally there will be data points above and below this point and a line with a slope of one (76). If the slope is less than one, the standard has a higher efficiency of PCR amplification. Conversely, if the slope is greater than one, the target has a higher efficiency of PCR amplification. This strategy was employed to develop a Competitive RT-PCR assay that was capable of measuring A1 transcripts in the range of 1 to 50 pg when 2.5μg of total RNA was added.

Table 1. Death Receptor Gene Family. Indicated below are members of the Death Receptor Gene Family, homologues for each gene, and the putative ligand that binds to the death receptor.

Gene	Homologue	Death Ligand
Fas	Apo1, Cd95, APT1	FasL (CD95L)
TNF-R1	CD120a, p55-R, TNFAR, TNFR60	TNF
DR3	APO-3, TRAMP, WSL-1, LARD	TWEAK (DR3L, Apo3L)
DR4	Apo2, TRAIL-R1	TRAIL (Apo2L)
DR5	TRAIL-R2, KILLER, TRICK2A, TRICKB	TRAIL (Apo2L)
DR6	TR7	unknown

Locksley, 2001
Ozoren N, 2003

Table 2. Adaptor Gene Family. Indicated below are several members of the Adaptor Gene Family and their putative function in the apoptosis signaling pathway.

Gene	Function
FADD	Interacts with Fas to promote apoptosis
TRADD	Interacts with TNF-R1 and recruits FADD to promote apoptosis
RIP	Recruited through TRAF2 and implicated in NFkB inhibition of apoptosis
FLIP	Interacts with DISC to prevent Caspase-8 activation and inhibition of apoptosis
TRAF2	Stimulate pathways that activate MAPK, which can promote or inhibit apoptosis

Ozoren N, 2003
Schulze-Osthoff, 1998
Gupta S, 2003
Krueger A, 2001

Table 3. Caspase Gene Family. Indicated below are the 14 members of the Caspase Gene Family, the homologues of each caspase, and the putative function of each caspase. In addition, the sequence of amino acids that represent the proteolytic cleavage site in target proteins is indicated for each caspase.

Gene	Homologue	Function	Cleavage Site
Caspase-1	ICE	Cytokine Activation	W/Y EHD
Caspase-2	ICH-1, Nedd2	Apoptosis Initiator	DEHD
Caspase-3	CPP32, Yama, Apopain	Apoptosis Effector	DEHD
Caspase-4	ICErel II, TX, ICH-2	Cytokine Activation	W/Y EHD
Caspase-5	ICErel III, TY	Cytokine Activation	W/Y EHD
Caspase-6	Mch2	Apoptosis Effector	I/L/V EHD
Caspase-7	Mch3, ICE-LAP3, CMH-1	Apoptosis Effector	DEHD
Caspase-8	FLICE, MACH, Mch5	Apoptosis Initiator	I/L/V EHD
Caspase-9	ICE-LAP6, Mch6	Apoptosis Initiator	I/L/V EHD
Caspase-10	Mch4	Apoptosis Initiator	I/L/V EHD
Caspase-11	ICH-3	Cytokine Activation	unknown
Caspase-12	unknown	Cytokine Activation	unknown
Caspase-13	ERICE	Cytokine Activation	unknown
Caspase-14	MICE	Cytokine Activation	W/Y EHD

Nicholson DW, et al., 1999
Ashe PC, et al., 2003
Salvesen GS, 2002

Table 4. Bcl-2 Gene Family. Indicated below are Anti-apoptotic and Pro-apoptotic members of the Bcl-2 Gene Family. The Bcl-2 homology domains (BH1, 2, 3, and 4) are indicated for each gene.

Anti-apoptotic

Gene	Domain(s)
Bcl-2	BH1, BH2, BH3, BH4
Bcl-XL	BH1, BH2, BH3, BH4
Bcl-w	BH1, BH2, BH3, BH4
Mcl-1	BH1, BH2, BH3, BH4
Boo/DIVA	BH1, BH2, BH3, BH4
A1/Bfl-1	BH1, BH2, BH3, BH4
NR-13	BH1, BH2, BH3, BH4

Pro-apoptotic

Gene	Domain(s)
Bax	BH1, BH2, BH3
Bak	BH1, BH2, BH3
Bok	BH1, BH2, BH3
Bcl-XS	BH3, BH4
Bid	BH3
Bad	BH3
Bik/Nbk	BH3
Bim/Bod	BH3
Blk	BH3
Hrk	BH3
Nix	BH3
BNip3	BH3
Noxa	BH3
PUMA	BH3
Bcl-rambo	BH1, BH2, BH3, BH4

Antonsson, 2001
Cory S, 2002

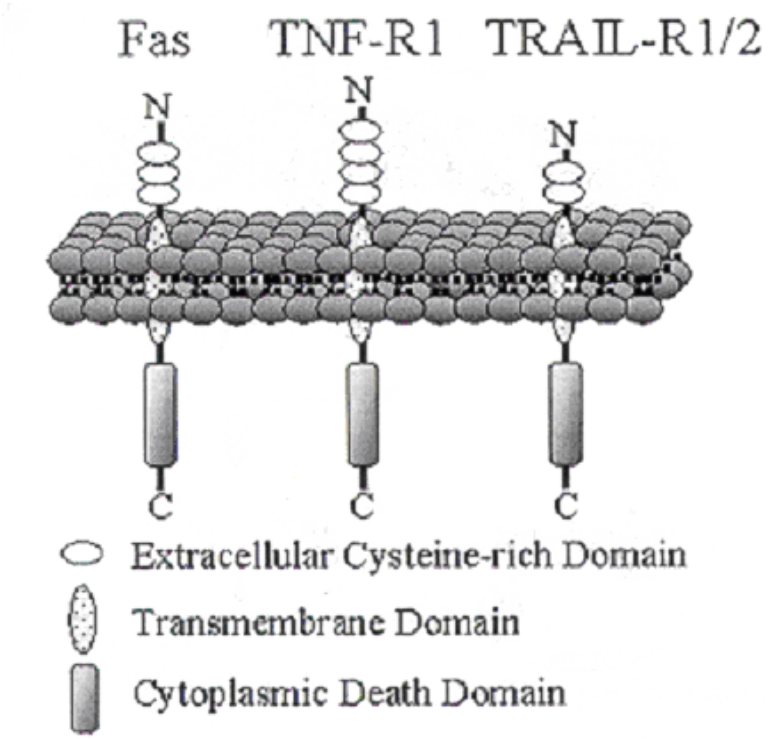

Figure 1. Structures of Death Receptors. Death receptors are type-I transmembrane proteins with an extracellular ligand-binding N-terminal region containing cysteine-rich domains, a membrane spanning region, and a C-terminal intracellular tail containing the death domain essential for signaling apoptosis. TNF-R1, tumor necrosis factor receptor 1; TRAIL-R1/2, tumor necrosis factor related apoptosis inducing ligand receptors 1 and 2. (Yoon J, 2002)

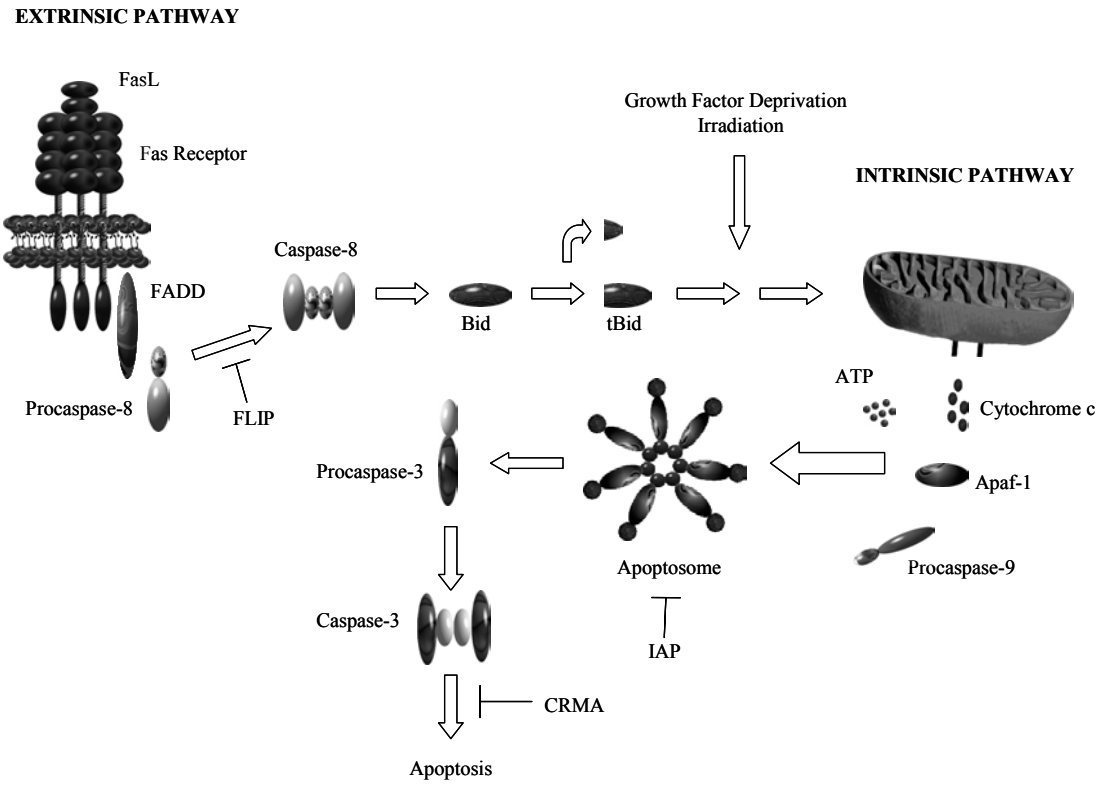

Figure 2. Extrinsic and Intrinsic Model of Apoptosis. In this example, the Fas death receptor mediates apoptosis. Following Fas Ligand binding to the Fas death receptors, the adaptor protein FADD interacts with Fas and initiates the activation of procaspase-8. In turn, Active caspase-8 cleaves Bid to form tBid, which can now act at the level of the mitochondria to promote the release of cytochrome c. Cytochrome c then combines with procaspase-9, Apaf-1, and ATP to form the apoptosome, which ultimately enables activation of the downstream caspases that execute apoptosis. Growth factor deprivation and Irradiation also activate the intrinsic pathway, while FLIP, IAP, and CRMA function as inhibitors of this signaling pathway.

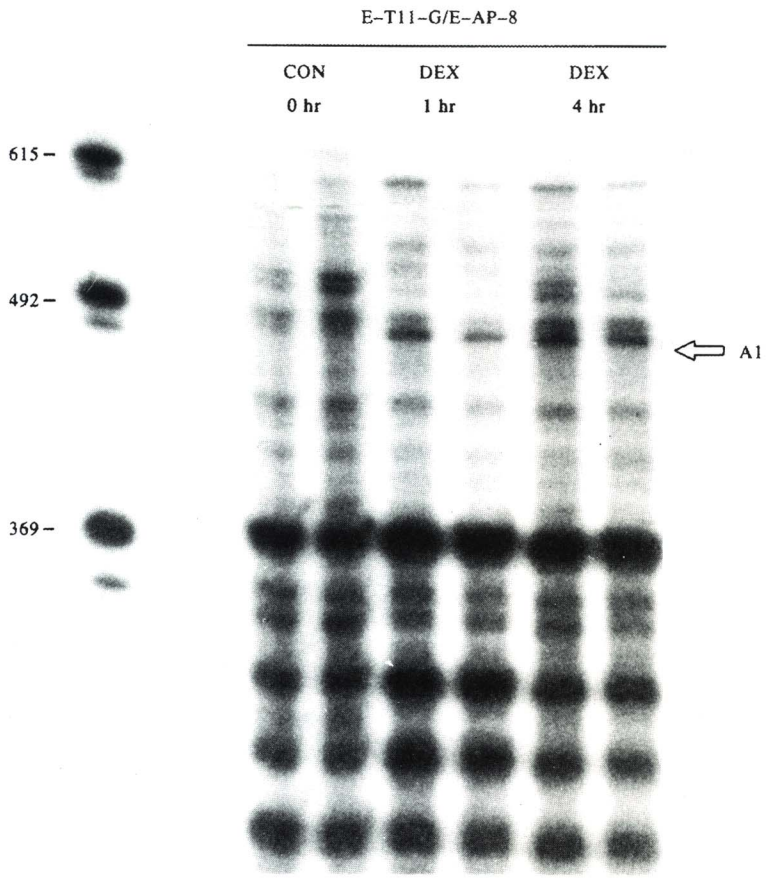

Figure 3. Differential Display Autoradiograph of A1. Enlargement of a portion of the differential display autoradiograph showing the expression of the differential display product, A1. The primer combination E-T11-G/E-AP-8 (underlined) was employed in the PCR amplification reaction. Differential display analysis was performed on duplicate RNA samples from chicken thymocytes treated in vitro for 0, 1 and 4 h with 1 μM dexamethasone. The differential display product A1 is indicated by an arrow on the right side of the figure. A radiolabeled 123 base pair marker is indicated on the left side of the figure. (Thomson JM, 1997)

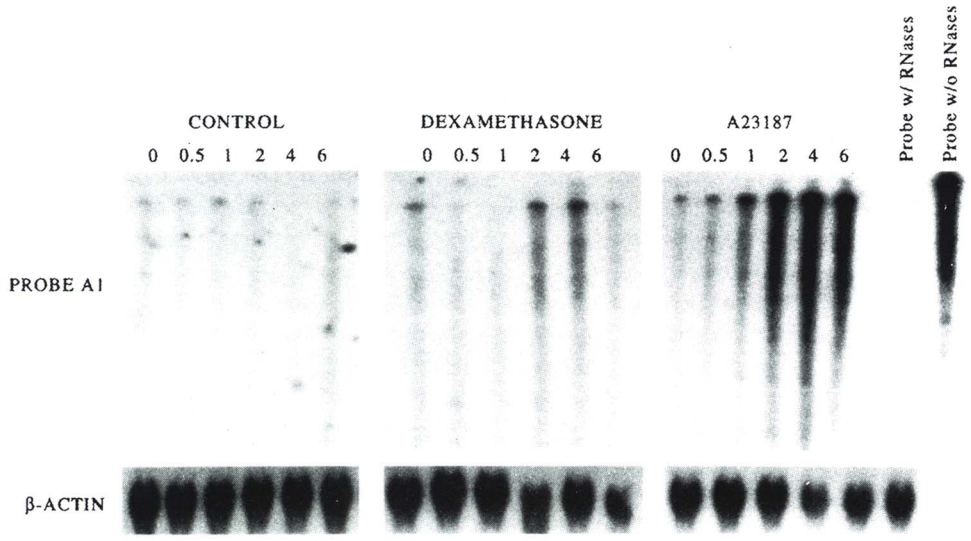

Figure 4. Ribonuclease Protection Analysis of A1. Ribonuclease protection analysis was performed using the radiolabelled A1 probe and RNA samples from chicken thymocytes treated in vitro for 0, 0.5, 1, 2, 4, and 6 h with a control vehicle, 1 μM dexamethasone and 1 μM A23187. Ribonuclease protection analysis of the radiolabelled A1 probe in the presence (probe w/RNases) or absence (probe w/o RNases) of added RNases is shown on the right side of the figure. Below the ribonuclease protection analysis is a Northern analysis of the corresponding samples using chicken beta-actin as a radiolabelled probe to confirm the normalization of RNA samples. These data are representative of three replicated experiments. (Thomson JM, 1997)

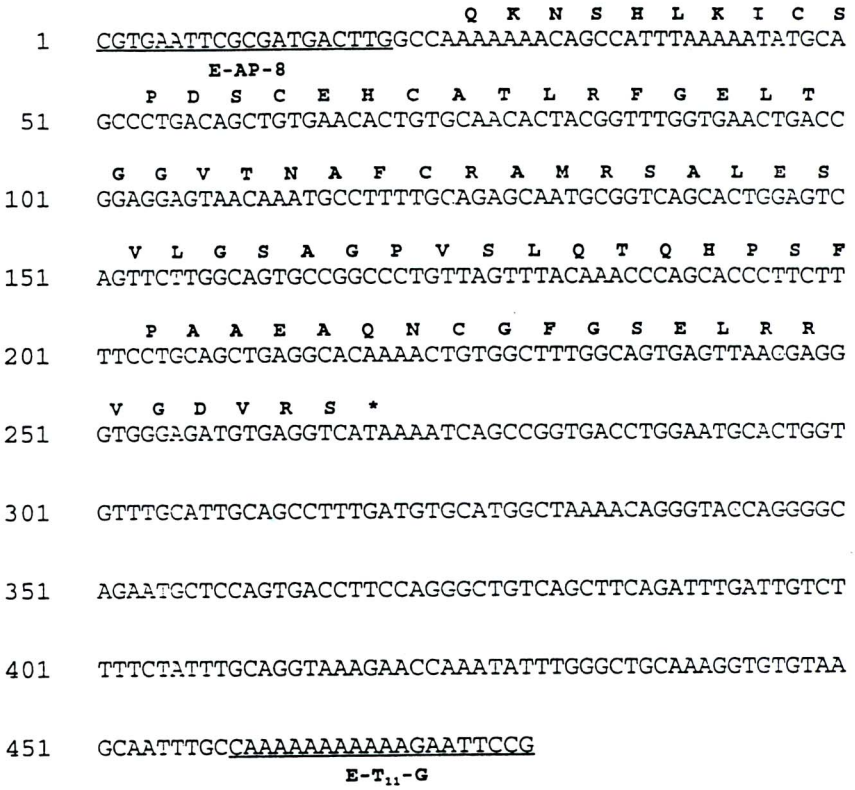

Figure 5. Nucleotide Sequence and Putative Open Reading Frame for A1. The nucleotide sequence of the A1 display product is shown above (GenBank accession number U93865). The gene fragment is 479 nucleotides in length and is presented in the sense orientation 5'-3' with the primer set E-AP-8 (modified arbitrary decamer) and E-T_{11}-G (modified degenerate oligo-dT) shown (underlined) flanking the amplified region. A putative open reading frame (ORF) consisting of 82 amino acids is indicated above the nucleotide sequence. The * indicates the putative stop codon. (Thomson JM, 1997)

A)

```
A1:      1 QKNSHLKICSPDSCEH...CATLR.....FGE.......LTGGVTNAFCR 35
           + +S ++I++ +++E+   +AT R     ++E        +G +++++ +
Bad:    39 AAQSMFQIPEFEPSEQEDASATDRGLGPSLTEDQPGPYLAPGLLGSNIHQ 88
                .         .         .         .         .
           36 AMRSALESVLGSAGPVSLQTQHPSFPAAEAQNCG..............  69
              + R+A +S  G+AG+++ +++H+S+PA+++++ G
           89 QGRAATNSHHGGAGAMETRSRHSSYPAGTEEDEGMEEELSPFRGRSRSAP 138
                .
           70 ........FGSELRRVGD 79
                     +G+ELRR++D
          139 PNLWAAQRYGRELRRMSD 156
```

B)

		BH1	
Bcl-2 (Human)	144	WGRIVAFFE-	152
Bax (Human)	107	WGRVVALFY-	115
Ced-9 (C.elegans)	168	YGRLIGLIS-	176
Bad (Mouse)	147	YGRELRRMSD	156
A1 (Chicken)	70	FGSELRRVGD	79

Figure 6. Analysis of the Putative Open Reading Frame of A1. (A) The Bestfit alignment of the 82 amino acid predicted ORF of A1 with the mouse protein, Bad. Identical amino acids are denoted by letters and the + denotes conservative amino acid substitutions. (B) The alignment of A1 with Bad and other Bcl-2 gene family members in the region of the BH1 domain. The underlined amino acids are highly conserved in this region. The flanking numbers denote amino acid positions of respective proteins and dashes in the amino acid sequence denote computer generated gaps that maximize alignment of the proteins. (Thomson JM, 1997)

CHAPTER 2

MATERIALS AND METHODS

Bursal Lymphocyte Cell Culture

Primary cultures of bursal lymphocytes were prepared from three-six week old broiler chicks as previously described (98). The tissue was aseptically removed from the chicken, minced in 4ºC DMEM (Dulbeco's Modified Eagle's Medium), and gently homogenized using a loose fitting, glass homogenizer. The tissue was then filtered through 100 μm nylon mesh, centrifuged at 1200 g for five minutes at 4ºC, and then resuspended in DMEM. These same filtration, centrifugation, and resuspension steps were repeated and the cell concentration was determined using a Coulter Counter Model F (Beckman Coulter, Fullerton, CA). The isolated lymphocytes were cultured in 80 mm petri dishes at 37ºC in a humidified 5% CO_2 atmosphere. The cells were cultured at a concentration of 1.5×10^6 cells/ml in 15 ml of DMEM supplemented with 5% heat-inactivated newborn calf serum, 5% heat-inactivated chicken serum, 4.5 mg/ml glucose, 50 μg/ml streptomycin sulfate, and 50 units/ml penicillin.

RNA Isolation

Total RNA was isolated from cultured cells (86) using the TRIZOL Reagent (Life Technologies, Gaithersburg, MD) according to the manufacturer's instructions. Approximately 2×10^7 lymphocytes were mixed with one ml of TRIZOL Reagent and centrifuged at 12,000 g for 10 minutes at 4ºC. The supernatant fraction was extracted with chloroform, followed by the addition of isopropyl alcohol to precipitate the RNA in

the aqueous fraction. The sample was centrifuged at 12,000 g for 10 minutes at 4ºC, and the RNA pellet was stored in 75 % ethanol at -20ºC. Prior to use, the RNA pellet was solubalized in nuclease-free water.

DNase Treatment

To remove contaminating DNA in the RNA samples, they were treated with DNase prior to the Competitive RT-PCR reaction (99). First, the samples were heated at 95ºC for three minutes in the presence of 0.1 mM EDTA to dissociate DNA/RNA hybrid strands and then chilled on ice for 3 minutes. The contaminating DNA was subsequently removed using a DNA-*free*™ kit (Ambion, Austin, TX). The samples (25-130 µg of RNA in a volume of 25 µl) were incubated in a DNase Enzyme Mixture (Ambion, Austin, TX) at 37ºC for one hour. To remove the DNase enzyme, 5 µl of the DNase Inactivation Reagent (Ambion, Austin, TX) were added and the samples were centrifuged for one minute at 10,000 g to pellet the inactivation reagent. The DNA-free RNA in the supernatant fraction was transferred into another tube and quantitated spectrophotometrically.

cDNA Synthesis

The initial step in the Competitive RT-PCR analysis was a reverse transcription reaction designed to produce cDNA (92). This step was performed using a 2.5 µg aliquot of DNA-free RNA sample that had a known amount (1, 10, or 50 pg) of the RNA standard added (the method for generation of the RNA standard is described below). The RNA template was combined with 0.25 µg oligo dT (T_{18}), 0.5 mM dNTP, and 1 µg random hexanucleotides, in a total reaction volume of 20 µl. The samples were then incubated at room temperature for 10 minutes, followed by 65ºC for five minutes and 4ºC

for two minutes. Subsequently, the samples were equilibrated at 42ºC for two minutes, and the following reagents were added to each sample: RT Synthesis Buffer (50 mM Tris-HCl pH 8.3, 75 mM KCl, 3 mM $MgCl_2$, and 10 mM DTT), 20 units RNasin (Promega, Madison, WI), and 100 units of Superscript II RNase H^- RT (Invitrogen, Carlsbad, CA). The reverse transcription reaction was performed by incubating the samples at 42ºC for 30 minutes, followed by 50ºC for 20 minutes and 70ºC for 15 minutes.

Polymerase Chain Reaction

Following the cDNA synthesis reaction, PCR amplification of the A1 transcripts was performed using the Hot Start PCR method (100). Each PCR reaction contained 20mM Tris-HCl (pH 8.4), 50 mM KCl, 15 mM $MgCl_2$, 0.2 mM dNTP, 5 µl of the newly generated cDNA, 5 units SureStart® *Taq* DNA Polymerase (Strategene, La Jolla, CA), 0.2 µM downstream primer, and 0.2 µM upstream primer, in a total reaction volume of 50 µl. PCR amplification involved an initial 15 minute incubation at 94°C to activate the Hot Start Taq Polymerase, followed by 30 cycles at 94°C for 30 seconds, 58°C for 30 seconds, and 68°C for two minutes. A final PCR cycle was performed at 68°C for five minutes. An Amplitron II (Barnstead Thermolyne Corporation, Dubuque, IO) thermocycler was used to execute all PCR reactions.

The primers used for PCR amplification were selected from the coding region of the A1 display product (69). The nucleotide sequence of the forward primer (A1.4/GSP/F) is 5'-AGTAACAAATGCCCTCTGC -3' and the reverse primer (GSP/A1/RT) is 5'-AAGGTCACTGGAGCATTCTG-3'. Using these primers, an A1 PCR product of 264 base pairs was generated and a 206 bp ΔA1 (standard) PCR product

was generated. Both of these primers were synthesized by the University of Georgia Molecular Genetics Instrumentation Facility, as were the primers used to generate the RNA standard for the Competitive RT-PCR assay.

Agarose Gel Electrophoresis

A 15 µl aliquot of the PCR reaction mixture was electrophoresed on a 2.5 % ethidium bromide stained agarose gel, and densitometric scanning of the agarose gel was performed using a Gel Doc 1000 Image Analysis System and Molecular Analyst software (BioRad Laboratories, Herculues, CA). The densitometric scanning was further used to obtain values for each agarose gel band, with the top band representing the transcript signal (T) and the bottom band representing the standard signal (S). For each sample, a T/S ratio was calculated and plotted on a double log graph against a known amount of the standard (1, 10, and 50 pg). Quantitation was then determined at the point where the target and the standard were equivalent.

Generation of the Competitive RNA Standard

For the quantitation of endogenous A1, an exogenous A1 transcript was needed to serve as a standard in the Competitive RT-PCR assay. To prepare the A1 standard, the A1 display product was cloned into a pGEM-T vector (Promega, Madison, WI) using a T/A cloning strategy (101). The plasmid DNA from the pGEM-T/A1 construct was subsequently isolated using the Wizard Plus Minipreps DNA Purification System (Promega, Madison, WI) and served as a template for generating the exogenous A1 standard (ΔA1) (Figure 7). Since A1 possesses an endogenous Bst E II restriction site at position 331, a second Bst E II restriction site was introduced at position 390 via PCR amplification using the conditions mentioned previously. Using the A1.4/GSP/F (5'-

AGTAACAAATGCCCTCTGC-3’) and GSPA1/BSTE (5’-AAGGTCACTGGAGCATTCTGCCCCTGGTCACCCTGTTTTAGCC-3’) primer combination, a C was added at position 393 to generate the second Bst EII restriction site (Figure 8). Consequently, a PCR product was generated that contained two Bst EII restriction sites spaced 58 nucleotides apart. This PCR product was then T/A cloned into a pGEM-T vector (Promega, Madison, WI) to create a pGEM-T/A1-BstEII construct. This construct was subsequently digested with Bst E II to remove the 58 bp intervening sequence and a ligation reaction was then performed to generate pGEM-T/ΔA1. This construct was subsequently linearized with Nco I and used as a template to generate a ΔA1 transcript using SP6 RNA Polymerase (Promega, Madison, WI). This ΔA1 competitor transcript is approximately 22% smaller than the endogenous A1 transcript.

Analysis of A1 Expression in Avian Tissues

To analyze A1 expression in various avian tissues, approximately 100 mg of each tissue (bursa, thymus, brain, spleen, kidney, heart, liver, testes, breast muscle, pancreas, small intestine) were collected from three-six week old broilers and immediately homogenized in the TRIZOL Reagent (Life Technologies, Gaithersburg, MD). Following RNA isolation, each tissue was treated with RNase-free DNase. RNA samples (2.5 μg) were reverse transcribed in the presence of 1, 10, or 50 pg of ΔA1. PCR was performed to amplify the cDNA and agarose gel electrophoresis was used to analyze the A1 and ΔA1 PCR products. The expression of A1 was quantitated by plotting the T/S ratio for each dose of the ΔA1 standard. Three replicates of each tissue sample were performed using three separate birds.

Time Course of A1 Expression in Cultured Bursal Lymphocytes

A time course (0, 1, 2, 4, 6, and 8 hours) was performed to examine the expression of A1 in cultured bursal lymphocytes undergoing apoptosis. Primary cultures of bursal lymphocytes were prepared from three separate birds as previously described. For each time point, total RNA was isolated from triplicate cell culture dishes containing bursal lymphocytes that were pooled together from a single bird. The RNA samples were subsequently analyzed for A1 expression using the A1 Competitive RT-PCR assay. Thus, for each time point, A1 expression was analyzed in bursal lymphocytes generated from three separate birds and this experiment was performed two times.

Time Course of Cell Viability in Cultured Bursal Lymphocytes

A time course (0, 1, 2, 4, 6, and 8 hours) was performed to analyze cell viability in cultured bursal lymphocytes undergoing apoptosis. Primary cultures of bursal lymphocytes were prepared from three separate birds as previously described. For each time point, duplicate samples were obtained from one cell culture dish per bird. Bursal lymphocytes were subsequently stained with 0.1 % trypan blue in PBS for five minutes. One hundred cells were counted for each sample and the percentage of viable cells that excluded the dye was then ascertained. Hence, for each time point, bursal lymphocyte viability was determined for each of the three birds.

Time Course of Caspase-3 Activity in Cultured Bursal Lymphocytes

A time course (0, 1, 2, 4, 6, and 8 hours) was performed to analyze Caspase-3 activity in bursal lymphocytes undergoing apoptosis. Primary cultures of bursal lymphocytes were prepared from three birds as previously described. For each time

point, the cells (1.5 x 10^6 cells/ml in 15 ml of DMEM) from one culture dish per bird were lysed in a buffer containing 10 mM HEPES (pH 7.5), 5 mM $MgCl_2$, 1 mM EDTA, 0.1% CHAPS, 20 µg/ml leupeptin, 10 µg/ml pepstatin, 1 mM AEBSF, and 10 µg/ml aprotinin. The samples were centrifuged at 15,000 g for 15 minutes at 4°C and the supernatant fraction was recovered and stored at –20°C. Duplicate 10 µg aliquots of lysate were incubated for two hours at 37°C in an assay buffer containing the following: 100mM HEPES (pH 7.5), 5mM DTT, 10% sucrose, 0.1% CHAPS, and 16 µM caspase substrate (Ac-DEVD-p nitroaniline). The Lowry procedure (102) was used to determine the protein concentrations of the cell lysates, with bovine serum albumin as the protein standard. The relative amount of p-nitroaniline released as a result of caspase activity was quantitated by measuring the optical density at 400 nm. The caspase-3 activity was expressed as µM p-nitroaniline released per 10 µg cell lysate protein per hour. Thus, for each time point, Caspase-3 activity was analyzed in bursal lymphocytes generated from three separate birds.

Treatment of Bursal Lymphocytes with the Phorbol Ester PDBu

To analyze the effect of a phorbol ester on A1 expression, bursal lymphocytes were subjected to *in vitro* treatment with Phorbol Dibutyrate (PDBu) for 0-8 hours. Primary cultures of bursal lymphocytes were prepared from three separate birds and treated with 100 nm PDBu. For each time point, total RNA was isolated from triplicate cell culture dishes containing bursal lymphocytes that were pooled together from one bird. Subsequently, the RNA was analyzed using the A1 Competitive RT-PCR assay, where each time point was generated from three separate birds.

Statistical Analysis

The data are presented as the mean ± one standard deviation. ANOVA was performed using the General Linear Model, and Duncan's Multiple Range Test was used to determine statistically significant differences among the means. A P value of < 0.05 was considered significantly different.

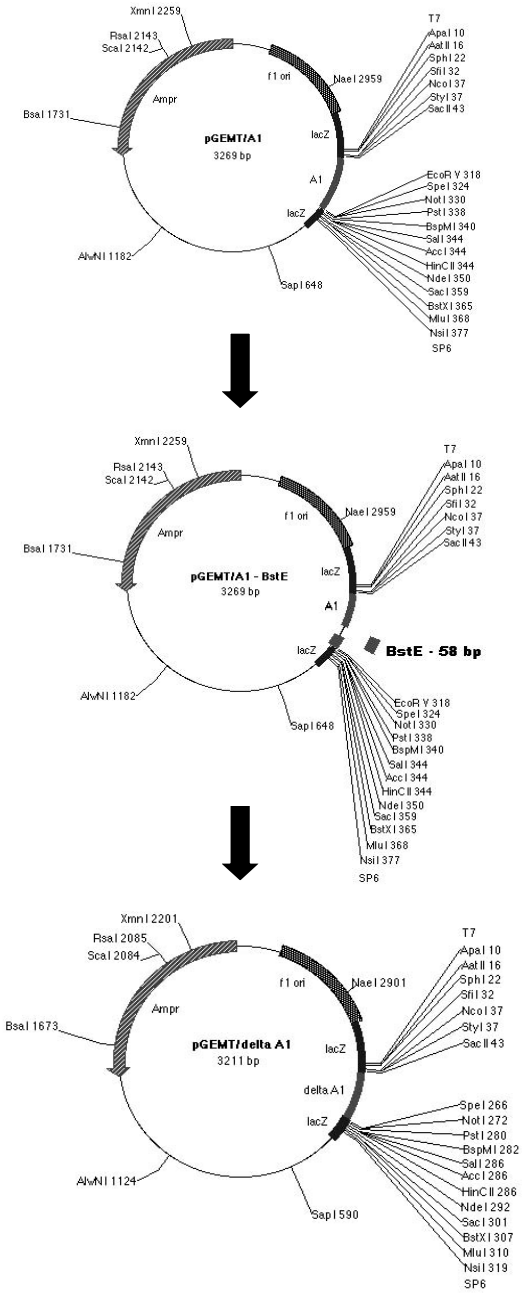

Figure 7. Generation of pGEMT/ΔA1 Construct. The A1 differential display product was ligated into the pGEMT vector to generate the pGEMT/A1 construct (upper panel). This construct was used as a template to generate the pGEMT/A1-Bst EII construct that contains 2 Bst EII sites in the A1 gene (middle panel). The pGEMT/A1-Bst EII plasmid was digested with Bst EII to remove the 58 bp fragment between the two Bst EII sites and religated to form the pGEMT/ΔA1 construct (bottom panel).

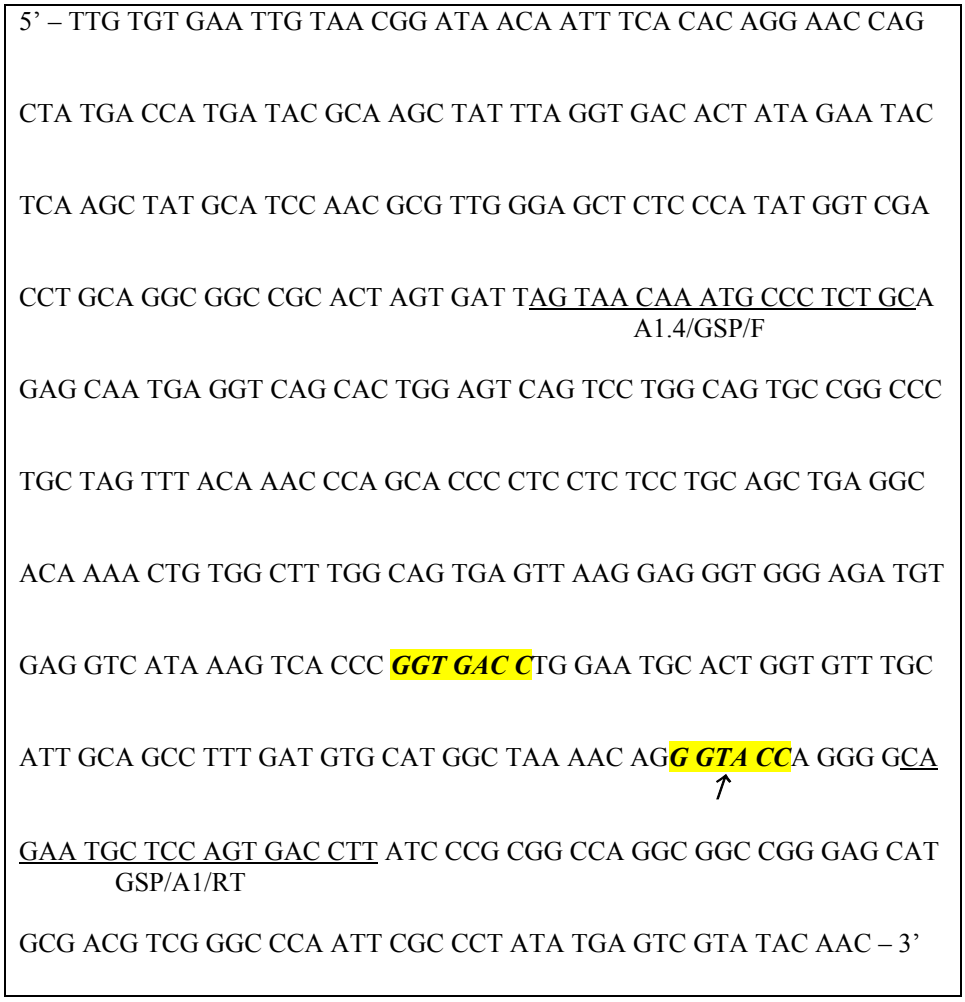

Figure 8. The Nucleotide Sequence of A1 Demonstrating the Generation of the ΔA1 Construct. The ΔA1 construct was generated by introducing a second Bst EII restriction site via PCR amplification and performing a restriction digest with the Bst EII enzyme. The arrow indicates where a C was added to create the new Bst EII restriction site. The 58 bp sequence between the two Bst EII restriction sites (highlighted) was removed to generate a construct termed ΔA1.

CHAPTER 3

RESULTS

Validation of Competitive RT-PCR Assay

To determine the optimal range of ΔA1 required for A1 quantitation in the described experiments, a 2.5 μg aliquot of total RNA isolated from bursal lymphocytes was coamplified with a dilution series of the ΔA1 standard (0, 0.5, 1, 10, 50, 100, and 1000 pg). As shown in Figure 9, the relative intensity of the ΔA1 standard signal increased as the target A1 signal decreased. This interaction is a function of the competition between the target and the standard for primer binding during PCR amplification. When 2.5 μg of total RNA are used in this assay, A1 can be quantitated from 0.5 pg to 1000 pg. The equivalence point, which is approximately 10 pg, is used to quantitate the amount of endogenous A1 mRNA. For the experiments described herein, 1, 10, and 50 pg of the ΔA1 standard were selected for the Competitive RT-PCR assay so that amounts above and below this relative equivalence point could be analyzed.

To further validate the Competitive RT-PCR assay, varying amounts (1, 2.5, and 5 μg) of total RNA from bursal lymphocytes were analyzed for the A1 transcript in the presence of 1, 10, and 50 pg of the ΔA1 standard (Figure 10). Similar to the dose response of ΔA1 in Figure 9, the same relationship exists between the standard and the target RNA; as the intensity of the ΔA1 signal increases, the target A1 RNA signal decreases. For each dose of total RNA, the amount of A1 was determined by calculating the T/S ratio (Target/Standard ratio) in the presence of 1, 10, and 50 pg of ΔA1. When 1,

2.5, and 5 µg of total RNA were analyzed by the Competitive RT-PCR assay, 2.9, 6.2, and 12.4 pg of A1 transcript were detected, respectively. These data demonstrate a proportional dose response for the amount of total RNA and the amount of A1 transcripts detected. Furthermore, these data indicate that 2.5 µg of total RNA was sufficient to analyze A1 transcripts over a range of 1 to 50 pg.

Since it is known that DNA contamination of RNA preparations may lead to erroneous quantitation of transcripts using the Competitive RT-PCR assay, a DNase treatment protocol was developed to test its effectiveness at removing DNA in RNA samples (data not shown). The results revealed that contaminating DNA was virtually eliminated when RNA was treated with RNase-free DNase. Several controls were consistently implemented throughout the experiments to confirm that the Competitive RT-PCR assay was quantifying only A1 RNA transcripts and not contaminating DNA. These controls included samples that were treated with and without DNase, and the cDNA synthesis reaction was performed in the presence and absence of reverse transcriptase.

Expression of the A1 Gene in Avian Tissues

The A1 Competitive RT-PCR assay was used to analyze the relative level of A1 expression in various tissues. As shown in Table 5, the levels of A1 expression in all tissues examined were either below or near the threshold of detection using the A1 Competitive RT-PCR assay. In the bursa, thymus, testes, and small intestine (jejunum), less than 1 pg of A1 was detected; whereas, in the breast muscle approximately 1 pg of A1 was detected. Conversely, the A1 transcript was undetectable in the kidney, heart, brain (cerebrum), liver, pancreas, and spleen.

Time Course of A1 Expression in Cultured Bursal Lymphocytes

A time course experiment was performed to examine the expression of A1 in cultured bursal lymphocytes undergoing apoptosis. In this model, apoptosis is activated by an endogenous mechanism when these lymphoid cells are isolated from the intact bursal environment (103). Bursal lymphocytes were cultured *in vitro* for 0, 1, 2, 4, 6, and 8 hours and the isolated RNA was analyzed using the A1 Competitive RT-PCR assay (Figure 11). After 1 hour of incubation, A1 expression was elevated over five-fold compared to levels at 0 hour. The expression of A1 then declined at 2, 4, 6, and 8 hours to levels below those detected at 1 hour.

Time Course of Cell Viability in Cultured Bursal Lymphocytes

To examine the viability of cultured bursal lymphocytes over this time course, cell viability was determined using the trypan blue exclusion assay as previously described (103). These results (Figure 12) indicate that the cells were over 95 % viable from 0 to 6 hours; however, a decline in cell viability was noted at 6 (88%) and 8 (86%) hours. This decline in lymphocyte viability at 6 and 8 hours may correspond to changes associated with cells undergoing the latter stages of apoptosis. However, the cell viability remained high during the first several hours of incubation period when A1 expression dramatically increased.

Time Course of Caspase-3 Activity in Cultured Bursal Lymphocytes

To validate that the lymphocytes were actually undergoing apoptosis in these experiments, a Caspase-3 assay was performed, since expression of this proteolytic enzyme is considered to be a hallmark of apoptosis (4). Bursal lymphocytes were

collected from three birds and grown in cell culture for 0 to 8 hours. Following the incubation period, cell lysates were prepared and Caspase-3 activity was determined (Figure 13). The relative level of Caspase-3 activity is low at 0 hour and increases approximately six-fold at 1 hour. From 2-8 hours, Caspase-3 activity remained at levels approximately 9-12 fold higher than levels detected at 0 hour. These results clearly indicated that the cells were undergoing apoptosis in these time course experiments.

Treatment of Bursal Lymphocytes with the Phorbol Ester PDBu

Bursal lymphocytes were treated *in vitro* with Phorbol Dibutyrate (PDBu), a known inhibitor of apoptosis, to examine the effect of this agent on A1 expression. As shown in Figure 14, A1 expression was elevated after 1 hour of PDBu treatment and maintained this relative level of expression after 4, 6, and 8 hours of treatment. The pattern of A1 expression following PDBu treatment is markedly different when compared to cells that lack this treatment (Figure 11). After 1 hour of phorbol ester treatment, A1 expression was elevated approximately two-fold (15 pg); whereas, in the absence of this treatment, A1 expression was elevated approximately five-fold (26 pg). Thus, it would appear that PDBu treatment may blunt the elevated expression of A1 that was detected in the absence of this treatment.

Table 5. Analysis of A1 Expression in Avian Tissues. The Competitive RT-PCR assay was used to analyze the level of A1 expression in a 2.5 μg aliquot of total RNA from various avian tissues. These data are representative of 3 separate birds.

Tissue	**Level of A1 (pg)**
Bursa	< 1
Thymus	< 1
Brain	Undetectable
Spleen	Undetectable
Kidney	Undetectable
Heart	Undetectable
Liver	Undetectable
Testes	< 1
Breast Muscle	1.24
Pancreas	Undetectable
Small Intestine	< 1

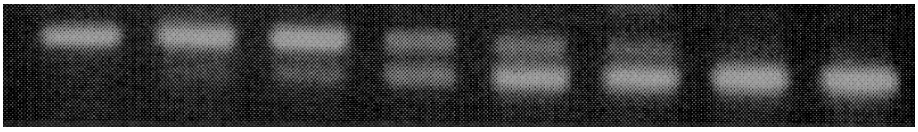

ΔA1 (pg) 0 0.5 1.0 10 50 100 500 1000

Figure 9. Dose Response of the ΔA1 Standard in the Competitive RT-PCR Assay. The ethidium bromide stained agarose gel shown above demonstrates the competition for PCR amplification between the target A1 transcript (upper band) and the ΔA1 standard (lower band). Total RNA (2.5 µg) isolated from bursal lymphocytes was coamplified with various amounts of ΔA1 (0, 0.5, 1, 10, 50, 100, or 1000 pg). For this sample, the ratio between the target and standard was equivalent at approximately 10 pg.

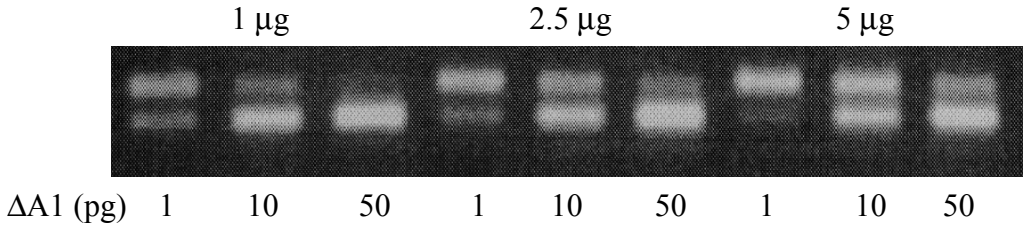

Figure 10. Dose Response of Total RNA in the Competitive RT-PCR Assay. The ethidium bromide stained agarose gel shown above further demonstrates the competition for PCR amplification between the target A1 transcript (upper band) and the ΔA1 standard (lower band). The ΔA1 standard (1, 10, or 50 pg) was coamplified with varying amounts of total RNA (1, 2.5, or 5 µg) isolated from bursal lymphocytes. In this dose response experiment, 2.9, 6.2, and 12.4 pg of the A1 transcript were detected in 1, 2.5, and 5 µg of total RNA, respectively.

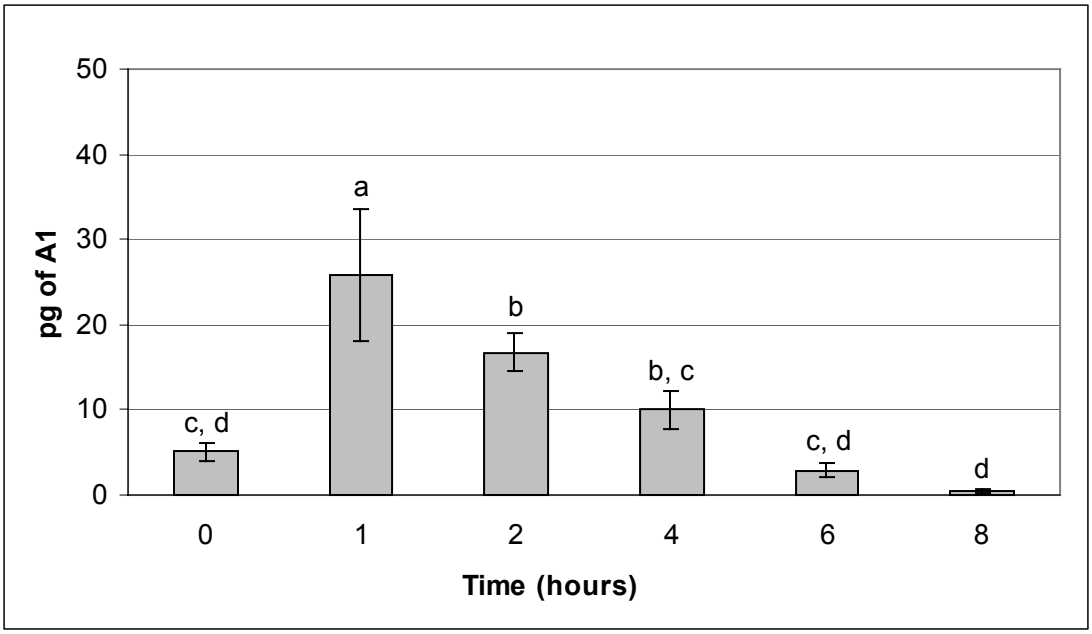

Figure 11. Time Course of A1 Expression in Cultured Bursal Lymphocytes. Freshly isolated bursal lymphocytes were cultured *in vitro* for 0, 1, 2, 4, 6 and 8 hours. Total RNA was then isolated and analyzed using the Competitive RT-PCR assay. The level of A1 expression is expressed in picograms on the Y-axis. The data represent the means ± 1 standard deviation from six birds in two separate experiments. Means having different letters (a-d) indicate a significant difference at the $P < 0.05$ level.

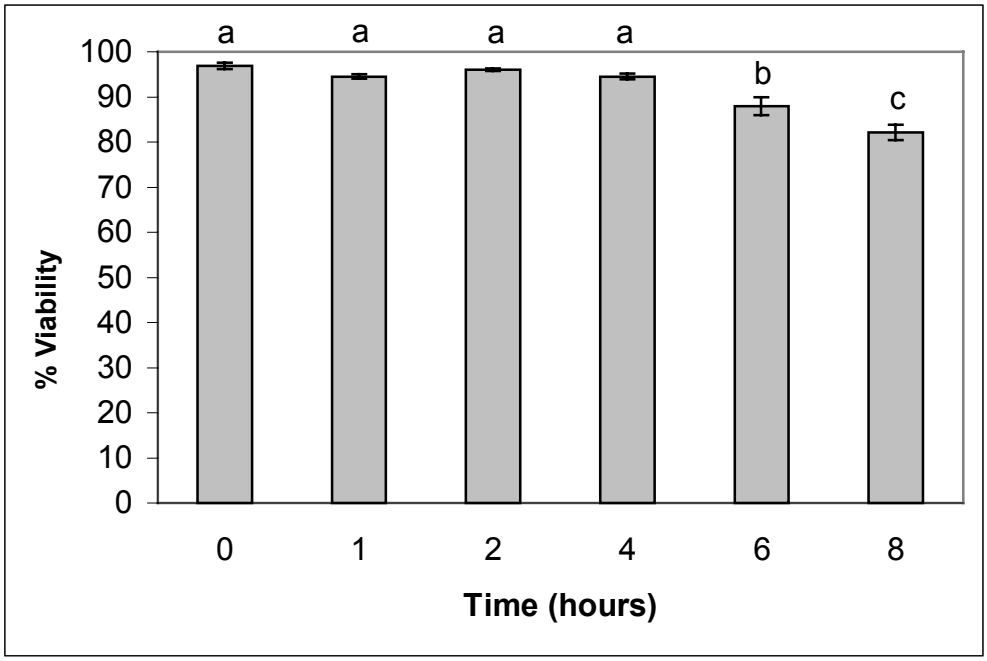

Figure 12. Time Course of Cell Viability in Cultured Bursal Lymphocytes. Freshly isolated bursal lymphocytes were cultured *in vitro* for 0, 1, 2, 4, 6, and 8 hours. The cells were then analyzed for cell viability using a trypan blue exclusion assay. The percentage of viable cells is shown on the Y-axis. The data represent the means ± 1 standard deviation from three birds. Means having different letters (a-c) indicate a significant difference at the $P < 0.05$ level.

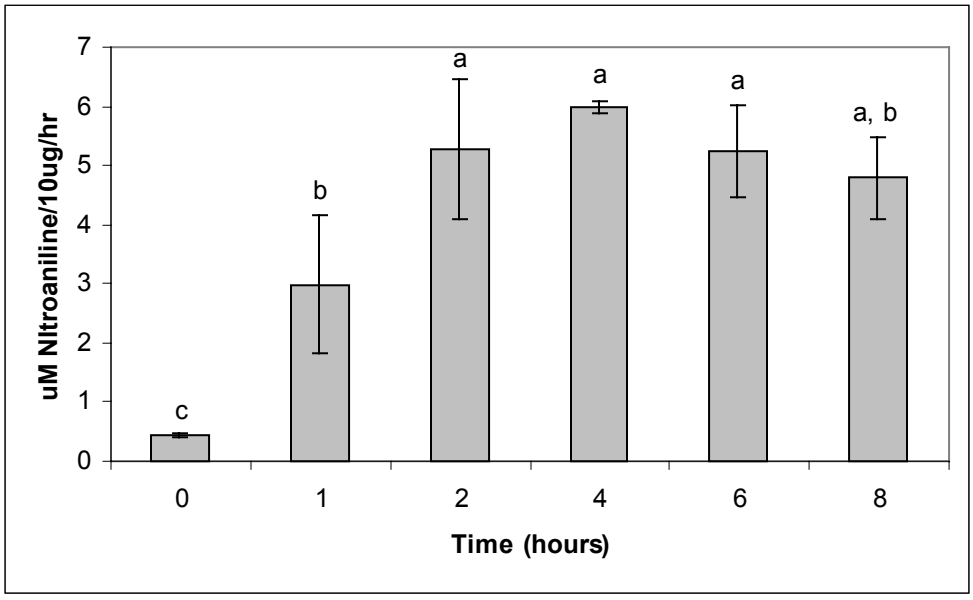

Figure 13. Time Course of Caspase-3 Activity in Cultured Bursal Lymphocytes. Freshly isolated bursal lymphocytes were cultured *in vitro* for 0, 1, 2, 4, 6, and 8 hours. Cell lysates were prepared and Caspase-3 enzyme activity was determined. The results are presented as µM Nitroaniline/10µg lysate protein/hr on the Y-axis. The data represent the means ± 1 standard deviation from three birds. Means having different letters (a-c) indicate a significant difference at the $P < 0.05$ level.

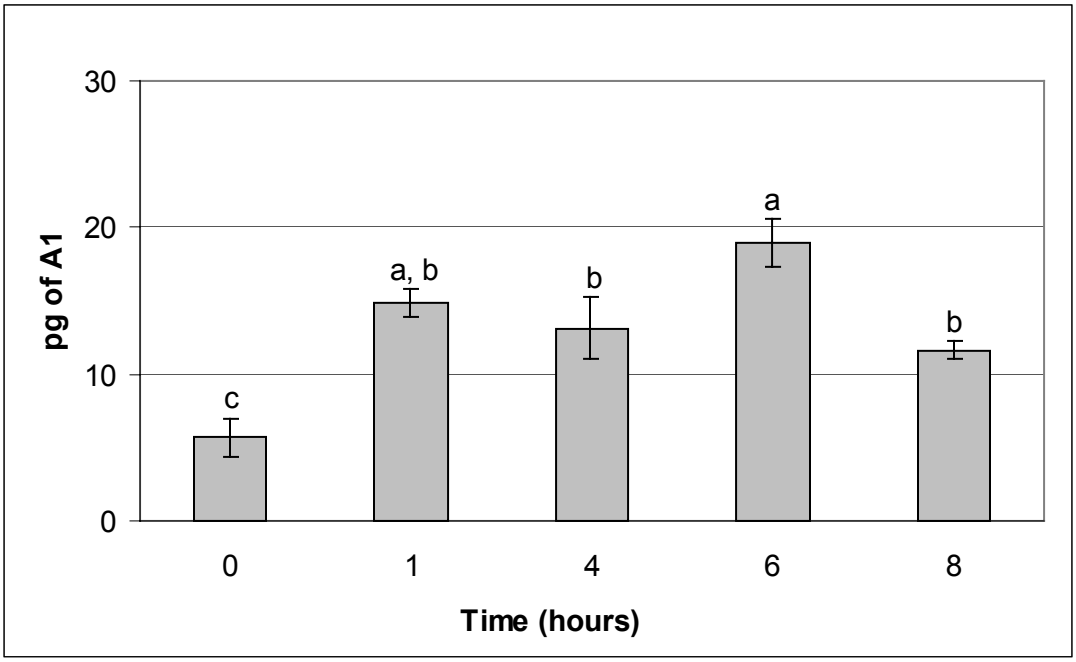

Figure 14. Treatment of Bursal Lymphocytes with PDBu. Freshly isolated bursal lymphocytes were cultured *in vitro* for 0, 1, 4, 6 and 8 hours in the presence of 100 nm PDBu. Total RNA was then isolated and analyzed for A1 expression using the Competitive RT-PCR assay. The level of A1 expression is expressed in picograms on the Y-axis. The data represent the means ± 1 standard deviation from three birds. Means having different letters (a-c) indicate a significant difference at the $P < 0.05$ level.

CHAPTER 4

DISCUSSION

A1 was initially identified as a differential display product that was detected in thymocytes undergoing apoptosis (69). When A1 expression was analyzed via a ribonuclease protection assay, elevated levels of A1 transcripts were detected near the onset of thymocyte apoptosis and continued to increase as a function of time. In the current study, a Competitive RT-PCR assay was developed to analyze A1 expression in bursal lymphocytes undergoing apoptosis. This sensitive assay can readily detect picogram levels of A1 transcripts (Figures 9 and 10). Furthermore, the *in vitro* culture of bursal lymphocytes represents an ideal model to analyze A1 expression in apoptotic cells. This primary cell culture system maintains a relatively high level of cell viability over the 8 hour time course in which cells are analyzed (Figure 12), and cells that are undergoing apoptosis express Caspase-3 activity, a definitive marker of apoptosis (Figure 13) (103, 104).

When the Competitive RT-PCR assay was used to analyze the expression of A1 in various avian tissues, the levels of A1 transcripts were either very low or virtually undetectable (Table 5). This finding is consistent with the concept that A1 expression is associated with the onset of apoptosis. Since the cells in these tissues were not undergoing apoptosis, the levels of A1 transcripts were very low. Conversely, basal levels of A1 expression in cultured bursal lymphocytes were higher than the levels detected in freshly collected whole tissues. These higher levels of A1 expression may

reflect the activation of apoptosis in a small population of cells during the lymphocyte isolation procedure.

When A1 expression was analyzed in bursal lymphocytes undergoing apoptosis over an eight hour time course, there was a dramatic elevation of A1 transcripts after one hour of incubation (Figure 11). This observation is similar to that noted for the time course of thymocyte apoptosis (69) and is consistent with the hypothesis that A1 expression is associated with the activation of apoptosis. However, this initial surge in A1 expression is followed by a rapid decline in the level of these transcripts at 2 and 4 hours. This pattern of A1 expression may indicate that it is a transient signal that activates apoptosis or it is a message that is rapidly degraded as a function of time in cells undergoing apoptosis. In contrast, A1 expression in thymocytes appears to increase as a function of the apoptotic process (69).

The signaling mechanism that initiates the endogenous activation of apoptosis in cultured bursal lymphocytes is unknown. However, one potential explanation for this phenomenon is that isolated bursal lymphocytes lack the stimulation by paracrine factors that are secreted from the bursal epithelium. This concept is supported by studies with prostatic epithelial cells and uterine epithelial cells that undergo apoptosis in the absence of gonadal steroids (105, 106). Furthermore, primary cultures of neurons die after the withdrawal of nerve growth factors (107). Thus, the deprivation of paracrine factors originating from the bursal epithelial may be a critical signal that activates A1 expression and initiates the apoptotic cascade in bursal lymphocytes.

Assuming that a surge in A1 expression is a potent activator of apoptosis, then it would be predicted that agents that protect cells from undergoing apoptosis would

moderate the expression of A1. The phorbol ester PDBu has previously been shown to inhibit apoptosis in this model system (103). In this study, the magnitude of A1 expression at 1 hour was blunted when bursal lymphocytes were subjected to PDBu treatment, suggesting that phorbol esters can activate signaling pathways that regulate A1 expression and activation of apoptosis. Previous research has shown that PDBu activates the protein kinase C-signaling pathway (108). It performs this action by directly binding to protein kinase C without the involvement of cell surface receptor components. In addition, PDBu also binds to calcium and phosphotidylserine to form an activated protein kinase complex. This complex then initiates a protein phosphorylation cascade that allows phosphorylation of transcriptional factors that alter gene expression, and consequently, alters cellular function (109). Previous research suggests that a protein kinase C pathway mediates the endogenous activation of bursal lymphocytes (103). Since the expression of A1 was increased following endogenous activation of apoptosis and was moderated when treated with PDBu, A1 may also be influenced by the protein kinase C pathway.

The data presented herein indicate that A1 plays a role in the activation of apoptosis in bursal lymphocytes. Since A1 expression may be implicated in the early phases of apoptosis, it may act at the level of the death receptors to activate the apoptotic process. Further elucidation of the functional role of A1 in apoptosis will require the isolation of full length cDNAs that encode A1. This data may help to identify homologues whose cellular function has been previously characterized.

REFERENCES

1. Marsden VS, Strasser A, 2003. Control of Apotosis in the Immune System. *Annual Review of Immunology* 21: 71-105.

2. Baehrecke EH, 2002. How Death Shapes Life During Development. *Nature Reviews Molecular Biology* 3: 779-787.

3. Bullock AN, Fersht AR, 2001. Rescuing the Function of Mutant p53. *Nature Reviews Cancer* 1: 68-76.

4. Geske FJ, Gerschenson LE, 2001. The Biology of Apoptosis. *Human Pathology* 32 (10): 1029-1035.

5. Welburn SC, Dale C, Ellis D, Beecroft R, Pearson TW, 1996. Apoptosis in procyclic Trypanosoma brucei rhodesiense in vitro. *Cell Death and Differentiation* 3: 229-236.

6. Ameisen JC, 1996. The origin of programmed cell death. *Science* 272 (5266): 1278-1279.

7. Lee N, Bertholet S, Debrabant A, Muller J, Duncan R, Nakhasi HL, 2002. Programmed cell death in the unicellular protozoan parasite Leishmania. *Cell Death and Differentiation* 9: 53-64.

8. Arnoult D, Akarid K, Grodet A, Petit PX, Estaquier J, Ameisen JC, 2002. On the evolution of programmed cell death: apoptosis of the unicellular eukaryote Leishmania major involves cysteine proteinase activation and mitochondrion permeabilization. *Cell Death and Differentiation* 9: 65-81.

9. Debrabant A, Lee N, Bertholet S, Duncan R, Nakhasi HL, 2003. Programmed cell death in trypanosomatids and other unicellular organisms. *International Journal for Parasitology* 33: 257-267.

10. Kerr JFR, Wyllie AH, Curie AR, 1972. Apoptosis: A basic biological phenomenon with wide ranging implications in tissue kinetics. *British Journal of Cancer* 26: 239-257.

11. Fishelson Z, Attali G, Mevorach D, 2001. Complement and Apoptosis. *Molecular Immunology* 38: 207-219.

12. Saraste A, Pulkki K, 2000. Morphological and biochemical hallmarks of apoptosis. *Cardiovascular Research* 45: 528-537.

13. Wyllie AH, 1997. Apoptosis: An overview. *British Medical Bulletin* 53: 451-465.

14. Nagata S, 1997. Apoptosis by death factor. *Cell* 88: 355-365.

15. Wyllie, AH, Kerr JFR, Currie AR, 1980. Cell death: The significance of apoptosis. *International Reviews in Cytology* 68: 251-306.

16. Liu X, Zou H, Slaughter C, Wang X, 1997. DFF, a heterodimeic protein that functions downstream of caspase-3 to trigger DNA fragmentation during apoptosis. *Cell* 89: 175-184

17. Enari M, Sakahira H, Yokoyama H, Okawa K, Iwamatsu A, Nagata SA, 1998. Caspase-activated DNase that degrades DNA during apoptosis and its inhibitor ICAD. *Nature* 391: 43−50.

18. Turner C, Devitt A, Parker K, MacFarlane M, Gluliano M, Cohen GM, Gregory CD, 2003. Macrophage-mediated clearance of cells undergoing caspase-3 independent death. *Cell Death and Differentiation* 10 (3): 302-312.

19. Strasser A, O'Conner L, Dixit V, 2000. Apoptosis signaling. *Annual Reviews of Biochemistry* 69: 217-245.

20. Budd RC, 2001. Activation-induced cell death. *Current Opinion in Immunology* 13: 356-362.

21. Yoon J, Gores GJ, 2002. Death receptor-mediated apoptosis and the liver. *Journal of Hepatology* 37: 400-410.

22. Ozoren N, El-Deiry WS, 2003. Cell surface Death Receptor signaling in normal and cancer cells. *Seminars in Cancer Biology* 13: 135-147.

23. Schulze-Osthoff K, Ferrari D, Los M, Wesselborg S, Peter ME, 1998. Apoptosis signaling by death receptors. *European Journal of Biochemistry* 254: 439-459.

24. Locksley RM, Killeen N, Lenardo MJ, 2001. The TNF and TNF Receptor Superfamilies: Integrating Mammalian Biology. *Cell* 104: 487-501.

25. Jordan MS, Singer AL, Koretzky GA, 2003. Adaptors as central mediators of signal transduction in immune cells. *Nature Immunology* 4 (2): 110-116.

26. Gupta S, 2003. Molecular signaling in death receptor and mitochondrial pathways of apoptosis (Review). *International Journal of Oncology* 22: 15-20.

27. Krueger A, Baumann S, Krammer PH, Kirchhoff S, 2001. FLICE-Inhibitory Proteins: Regulators of Death Receptor-Mediated Apoptosis. *Molecular and Cellular Biology* 21 (24): 8247-8254.

28. Lockshin RA, Zakeri Z, 2002. Caspase-independent cell deaths. *Current Opinion in Cell Biology* 14: 727-733.

29. Salvesen GS, 2002. Caspases and apoptosis. *Essays in Biochemistry* 38: 9-19.

30. Shi Y, 2002. Mechanisms of Caspase Activation and Inhibition during Apoptosis. *Molecular Cell* 9: 459-470.

31. Ashe PC, Berry MD, 2003. Apoptotic signaling cascades. *Progress in Neuro-Psychopharmacology & Biological Psychiatry* 27: 199-214.

32. Nicholson DW, 1999. Caspase structure, proteolytic substrates, and function during apoptotic cell death. *Cell Death and Differentiation* 6: 1028-1042.

33. Salvesen GS, Dixit VM, 1999. Caspase activation: the induced-proximity model. *Proceeding of the National Academy of Science U.S.A.* 96: 10964-10967.

34. van Loo G, Saelens X, van Gurp M, MacFarlane M, Martin SJ, Vandenabeele P, 2002. The role of mitochondrial factors in apoptosis: a Russian roulette with more than one bullet. *Cell Death and Differentiation* 9: 1031-1042.

35. Antonsson B, 2001. Bax and other pro-apoptotic Bcl-2 family "killer-proteins" and their victim, the mitochondrion. *Cell Tissue Research* 306: 347-361.

36. Cory S, Adams JM, 2002. The Bcl2 Family: Regulators of the Cellular Life-or-Death Switch. *Nature Reviews Cancer* 2: 647-656.

37. Yang E, Zha J, Jockel J, Boise LH, Thompson CB, Korsmeyer SJ, 1995. Bad, a heterodimeric partner for Bcl-x_L and Bcl-2, displaces Bax and promotes cell death. *Cell* 80: 285-291.

38. Wallach D, Varfolomeev EE, Malinin NL, Goltsev YV, Kovalenko AV, Boldin MP, 1999. Tumor Necrosis Factor Receptor and Fas Signaling Mechanisms. *Annual Review of Immunology* 17: 331-367.

39. Boldin MP, Varfolomeev EE, Pancer Z, Metl IL, Carmonis JH, Wallach D, 1995. A novel protein that interacts with the death domain of Fas/APO1 contains a sequence motif related to the death domain. *Journal of Biological Chemistry* 270: 7795-7798.

40. Kothakota S, Azuma T, Reinhard C, Klippel A, Tang J, Chu K, McGarry TJ, Kirschner MW, Koths K, Kwiatkowski DJ, Williams LT, 1997. Caspase-3 generated fragment of gelsolin: effector of morphological change in apoptosis. *Science* 278: 294-298.

41. Rao L, Perez D, White E, 1996. Lamin proteolysis facilitates nuclear events during apoptosis. *Journal of Cell Biology* 135: 1441-1455.

42. Wang J, Chun HJ, Wong W, Spencer DM, Lenardo MJ, 2001. Caspase-10 is an initiator caspase in death receptor signaling. *PNAS* 98 (24): 13884-13888.

43. Kischkel FC, Lawrence DA, Tinel A, LeBlanc H, Virmani A, Schow P, Gazdar A, Blenis J, Arnott D, Ashkenazi A, 2001. Death Receptor Recruitment of Endogenous Caspase-10 and Apoptosis Initiation in the Absence of Caspase-8*. *The Journal of Biological Chemistry* 276 (49): 46639-46646.

44. Scaffidi C, Fulda S, Srinivasan A, Friesen C, Li F, Tomaselli KJ, Debatin K, Krammer PH, Peter ME, 1998. Two CD95 (APO-1/Fas) signaling pathways. *The EMBO Journal* 17 (6): 1675-1687.

45. Li H, Zhu H, Xu CJ, Yuan J, 1998. Cleavage of BID by caspase-8 mediates the mitochondrial damage in the Fas pathway of apoptosis. *Cell* 94: 491-501.

46. Ravagnan L, Roumier T, Kroemer G, 2002. Mitochondria, the Killer Organelles and Their Weapons. *Journal of Cellular Physiology* 192: 131-137.

47. Grossmann J, 2002. Molecular mechanisms of "detachment-induced apoptosis-Anoikis." *Apoptosis* 7: 247-260.

48. Zamzami N, Marchetti P, Castedo M, Decaudin D, Macho A, Hirsch T, Susin SA, Petit PX, Mignotte B, Kroemer G, 1995. Sequential reduction of mitochondrial transmembrane potential and generation of reactive oxygen species in early programmed cell death. *Journal of Experimental Medicine* 182: 367-377.

49. Goldstein JC, Waterhouse NJ, Juin P, Evan GI, Green DR, 2000. The coordinate release of cytochrome c during apoptosis is rapid, complete and kinetically invariant. *Nature Cell Biology* 2: 156-162.

50. Fesik SW, 2000. Insights into programmed cell death through structural biology. *Cell* 103: 273-282.

51. Schendel SL, Azimov R, Pawlowski K, Godzik A, Kagan BL, Reed JC, 1999. Ion channel activity of the BH3 only Bcl-2 family member, BID. *Journal of Biological Chemistry* 274: 21932-21936.

52. Acehan D, Jiang X, Morgan DG, Heuser JE, Wang X, Akev CW, 2002. Three-dimensional structure of the apoptosome: implications for assembly, procaspase-9 binding, and activation. *Molecular Cell* 9: 423-432.

53. Martinou JC, Green DR, 2001. Breaking the mitochondrial barrier. *Nature Reviews in Molecular Cell Biology* 2: 63-67.

54. Demaurex N, Distelhorst C, 2003. Apoptosis-the Calcium Connection. *Science* 300: 65-67.

55. Pettus BJ, Chalfant CE, Hannun YA, 2002. Ceramide in apoptosis: an overview and current perspectives. *Biochimica et Biophysica Acta* 1585: 114-125.

56. Cuvillier O, 2002. Sphingosine in apoptosis signaling. *Biochimica et Biophysica Acta* 1585: 153-162.

57. Zhang J, Alter N, Reed JC, Borner C, Obeid LM, Hannun YA, 1996. Bcl-2 interrupts the ceramide-mediated pathway of cell death**.** *Proceedings of the National Academy of Sciences* 93: 5325-5328.

58. Tepper AD, de Vries E, van Blitterswijk WJ, Borst J, 1999. Ordering of ceramide formation, capase activation, and mitochondrial changes during CD95 and DNA damage induced apoptosis. *Journal of Clinical Investigation* 103 (7): 971-978.

59. Ruvolo PP, 2003. Intracellular signal transduction pathways activated by ceramide and its metabolites. *Pharmacological Research* 47: 383-392.

60. Burgess W, Jesse K, Tang Q, Broussard SR, Dantzer R, Kelley KW, 2003. Insulin-like growth factor-I and the cytokines IL-3 and IL-4 promote survival of progenitor myeloid cells by different mechanims. *Journal of Neuroimmunology* 15: 82-90.

61. Gottlieb E, Armour SM, Thompson CB, 2002. Mitochondrial respiratory control is lost during growth factor deprivation. *Proceedings of the National Academy of Sciences* 99 (20): 12801-12806.

62. Bortner CD, Cidlowski JA, 2002. Cellular Mechanisms for the Repression of Apoptosis. *Annual Review of Pharmacology and Toxicology* 42: 259-281.

63. Schuler M, Green DR, 2001. Mechanisms of p53-dependent apoptosis. *Biochemical Society Transactions* 29 (6): 684-688.

64. Yonish-Rouach E, Resnitzhy J, Lotem J, Sachs L, Kimchi A, Oren M, 1991. Wild-type p53 induces apoptosis of myeloid leukemic cells that is inhibited by interleukin-6. *Nature* 352: 345-347.

65. Dent P, Yacoub A, Contessa J, Caron R, Amorino G, Valerie K, Hagan MP, Grant S, Schmidt-Ullrich R, 2003. Stress and Radiation-Induced Activation of Multiple Intracellular Signaling Pathways. *Radiation Research* 159: 283-300.

66. Zhang W, Liu HT, 2002. MAPK signal pathways in the regulation of cell proliferation in mammalian cells. *Cell Research* 12 (1): 9-18.

67. Lin A, 2002. Activation of the JNK signaling pathway: breaking the break on apoptosis. *BioEssays* 25: 17-24.

68. Liang P, Zhu W, Zhang X, Guo Z, O'Connell RP, Averboukh L, Wang F, Pardee AB, 1994. Differential display using one-base anchored oligo-dT primers. *Nucleic Acid Research* 22: 5763-5764.

69. Thomson JM, Waldrip HW, Compton MM, 1997. Identification of a differential display product associated with apoptosis in chicken thymocytes. *Developmental and Comparative Immunology* 21: 413-424.

70. Lee JJ, Costlow NA, 1987. A molecular titration assay to measure transcript prevalence levels. *Methods in Enzymology* 152: 633-648.

71. Alwine JC, Kemp DJ, Stark GR, 1977. Method for detection of specific RNAs in agarose gels by transfer to diazobenzyloxymethyl-paper and hybridization with DNA probes. *Proceeding of the National Academy of Sciences USA* 74: 5350.

72. Costanzi C, Gillespie D, 1987. Fast blots: Immobilization of DNA and RNA from cells. *Guide to Molecular Cloning Techniques*. Academic Press, San Diego, CA.

73. Rappolee DA, Mark D, Banda MJ, Werb Z, 1991. *Science* 241: 708-712.

74. Kawasaki ES, 1991. *PCR Protocols: A Guide to Methods and Applications*. Academic Press, San Diego, CA.

75. Brenner CA, Tam AW, Nelson PA, Engelman EG, Suzukin, Fry KE, Larrick JW, 1989. Message Amplification Phenotyping (mapping) - a Technique to Simultaneously Measure Multiple Messanger-RNAs from Small Numbers of Cells. *BioTechniques* 7: 1096-1103.

76. Freeman WM, Walker SJ, Vrana KE, 1999. Quantitative RT-PCR: Pitfalls and Potential. *BioTechniques* 26: 112-125.

77. Becker-Andre M, Hahlbrock K, 1989. Absolute mRNA quantitation using the polymerase chain reaction (PCR). A novel approach by a PCR aided transcript titration assay (PATTY). *Nucleic Acids Research* 17: 9437-9446.

78. Gilliland G, Perrin S, Blanchard K, Bunn HF, 1990. Analysis of cytokine mRNA and DNA: detection and quantitation by competitive polymerase chain reaction. *Proceedings of the National Academy of Sciences USA* 87: 2725-2729.

79. Martorana AM, Zheng G, Springall F, Iland HJ, O'Grady RL, Lyons JG. 1999. Absolute Quantitation of Specific mRNAs in Cell and Tissue Samples by Comparative PCR. *BioTechniques* 27: 136-144.

80. Fille M, Shanley JD, Aslanzadeh J, 1997. Quantitative RT-PCR Using a PCR-Generated Competitive Internal Standard. *BioTechniques* 23 (1): 34-36.

81. Szibor M, Morawietz H, 2002. Serial Competitive RT-PCR Using Multiple Standards. *BioTechniques* 33 (4): 744-748.

82. Hayward-Lester A, Oefner PJ, Sabatini S, Doris PA, 1995. Accurate and absolute quantitative measurement of gene expression by single tube RT-PCR and HPLC. *Genome Research* 5: 494-499.

83. Siebert PD, Larrick JW, 1992. Competitive PCR. *Nature* 359: 557-558.

84. Higuchi R, Fockler C, Dollinger G, Watson R, 1993. Kinetic PCR analysis: real time monitoring of DNA amplification reactions. *BioTechnology* 11: 1026-30.

85. Chirgwin JM, Pryzbyla AE, MacDonald RJ, Rutter WJ, 1979. Isolation of biologically active ribonucleic acid from sources enriched in ribonuclease. *Biochemistry* 18: 5294.

86. Chomczynski P, Sacchi N, 1987. Single-step method of RNA isolation by acid-guandinium thiocyanate-phenol-chloroform extraction. *Analytical Biochemistry* 162: 156-159.

87. Matthews JLK, Chung M, Matyas JR, 2002. Persistnet DNA Contamination in Competitive RT-PCR Using cRNA Internal Standards: Identity, Quality, and Control. *BioTechniques* 32: 1412-1417.

88. McCulloch RK, Choong CS, Hurley DM, 1995. An evaluation of competitor type and size for use in the determination of mRNA by competitive PCR. *PCR Methods Applied* 4: 219-226.

89. Ferre F, 1992. Quantitative or semi-quantitative PCR: reality versus myth. *PCR Methods Applied* 2: 1-9.

90. Zimmermann K, Mannhalter JW, 1996. Technical aspects of quantitative competitive PCR. *BioTechniques* 21: 268-279.

91. Tang JQ, Lagace G, Collu R, 1996. Simple Method for Constructing Internal Standards for Competitive PCR. *BioTechniques* 21 (3): 378-380.

92**.** Krug MS, Berger SL, 1987. First-Strand cDNA Synthesis Primed with Oligo(dT). *Methods in Enzymology* 152: 316-325.

93. Choi I, Collisson EW, Maheswaran SK, Yoo HS, 2002. Evaluation of cytokine gene expression in porcine spleen cells, peripheral blood mononuclear cells, and alveolar macrophages by competitive RT-PCR. *FEMS Immunology and Medical Microbiology* 34: 119-126.

94. Erlich HA, Gelfand D, Sninsky JJ, 1991. Recent advances in the polymerase chain reaction. *Science* 252: 1643-1651.

95. Mullis KB, Faloona F, Scharf S, Saiki R, Horn G, Erlich H, 1986. Specific enzymatic amplification of DNA *in vitro* - the polymerase chain reaction. *Cold Spring Harbor Symposia on Quantitative Biology* 51: 263-273.

96. Dieffenbach CW, Lowe TMJ, Dveksler GS, 1993. General Concepts For PCR Primer Design. *PCR-Methods and Applications* 3 (3): S30-S37.

97. Farrell RE, Jr., 1998. *RNA Methodologies: A Laboratory Guide for Isolation and Characterization*, second edition. Academic Press, San Diego, CA.

98. Compton MM, Thomson JM, Icard AH, 2001. The analysis of cThy28 expression in avian lymphocytes. *Apoptosis* 6: 299-314.

99. Vanecko S, Laskowski M, 1961. Studies of the Specificity of Deoxyribonuclease I. *Journal of Biological Chemistry* 236: 3312-3316.

100. Birch DE, Kolmodin L, Laird WJ, McKinney N, Wong J, Young KKY, Zangenberg GA, Zoccoli MA, 1996. Simplified Hot Start PCR. *Nature* 381: 445-446.

101. Mezei LM, Storts DM, 1994. Cloning PCR Products. *PCR Technology: Current Innovations*, 21-27.

102. Lowry OH, Rosebrough NJ, Farr AL, Randall RJ, 1951. Protein Measurement with the Folin Phenol Reagent. *Journal of Biological Chemistry* 193 (1): 265.

103. Compton MM, Waldrip HM, 1998. Endogenous Activation of Apoptosis in Bursal Lymphocytes: Inhibition by Phorbol Esters and Protein Synthesis Inhibitors. *Cellular Immunology* 184: 143-152.

104. Compton MM, Wickliffe JK, 1999. Multiparametric Assessment of Bursal Lymphocyte Apoptosis. *Developmental and Comparative Immunology* 23: 487-500.

105. Rotello RJ, Lieberman RC, Lepoff GB, Gershenson LE, 1992. Characterization of Uterine Epethelium Apoptotic Cell Death Kinetics and Regulation by Progesterone and RU-486. *American Journal of Pathology* 140 (2): 449-456.

106. Kyprianou N, Isaacs JT, 1988. Activation of Programmed Cell Death in the Rat Ventral Prostate after Castration. *Endocrinology* 122 (2): 552-562.

107. Martin DP, Ito A, Horigome K, Lampe PA, Johnson EM, 1992. Biochemical-Characterization of Programmed Cell-Death in NGF-Deprived Symphathetic Neurons. *Journal of Neurobiology* 23 (9): 1205-1220.

108. Wender PA, Koehler KF, Sharkey NA, Dell Aquila ML, Blumberg PM, 1986. Analysis of the Phorbol Ester Pharmacophore on Protein-Kinase-C As a Guide to the Rational Design of New Classes of Analogs. *Proceedings of the National Academy of Sciences USA* 83 (12): 4214-4218.

109. Nishizuka Y, 1992. Intracellular Signalling by Hydrolysis of Phospolipids and Activation of Protein-Kinase-C. *Science* 258 (5082): 607-614.